

## CONTENTS G through I

---

Iron and Nickel in Ureilite Silicates — Chemistry and Isotopes <i>A. Gabriel, G. Quitté, R. Schönberg, J. Schüßler, and A. Pack</i> .....	5326
Spectroscopy and the Asteroid-Meteorite Link: A Perspective After Three Decades <i>M. J. Gaffey</i> .....	5357
Petrology and Geochemistry of the NWA 3368 Eucrite <i>K. G. Gardner, D. S. Lauretta, D. H. Hill, J. S. Goreva, K. J. Domanik, I. A. Franchi, and M. J. Drake</i> .....	5152
Composition in the Protosolar and Local Interstellar Clouds — Implications for the Chemical Evolution in the Galaxy During the Last 5 Gyr <i>J. Geiss and G. Gloeckler</i> .....	5134
Equilibrated Ordinary Chondrite-like Micrometeorites <i>M. J. Genge</i> .....	5070
Stable Iron Isotope Analyses of Metal Grains in Ordinary Chondrites by MC-ICP-MS <i>K. J. Gildea, R. Burgess, I. Lyon, and D. W. Sears</i> .....	5284
Iron Oxidation State in Australasian Micro-Tektites by High-Resolution XANES Spectroscopy and $K_{\beta}$ -detected XANES Spectroscopy <i>G. Giuli, S. G. Eeckhout, C. Koeberl, E. Paris, and G. Pratesi</i> .....	5150
Iron Oxidation State in Impact Glass from the Cretaceous/Tertiary Boundary at Beloc (Haiti) by High-Resolution XANES Spectroscopy: Implications on the Formation Conditions <i>G. Giuli, S. G. Eeckhout, C. Koeberl, G. Pratesi, and E. Paris</i> .....	5149
Divalent Vanadium in Vigarano CV3 Meteorite Chondrule <i>G. Giuli, G. Pratesi, S. G. Eeckhout, and E. Paris</i> .....	5148
The JaH 091 Strewfield <i>E. Gnos, M. Eggemann, A. Al-Kathiri, and B. A. Hofmann</i> .....	5112
The KREEP-rich Imbrium Impact Melt Breccia of the Lunar Meteorite Sayh Al Uhaymir 169 <i>E. Gnos, B. A. Hofmann, A. Al-Kathiri, and M. J. Whitehouse</i> .....	5111
Effects of Falling Impact Ejecta on the Post-Chicxulub Atmosphere <i>T. J. Goldin and H. J. Melosh</i> .....	5073
Constraining Volatile Abundance in Chondritic Components <i>S. H. Gordon, P. A. Bland, S. J. Hammond, and N. W. Rogers</i> .....	5213
Li-Be Isotope Systematic in Efremovka CAIs <i>J. N. Goswami and M. P. Deomurari</i> .....	5342
An $^{16}\text{O}$ CAI-like Particle Among Antarctic Micrometeorites <i>M. Gounelle, M. Chaussidon, C. Engrand, J. Duprat, and H. Leroux</i> .....	5279
Depth-dependant Fractionation of Light Solar Wind Noble Gases in a Genesis Target <i>A. Grimberg, F. Bühler, P. Bochsler, D. S. Burnett, H. Baur, and R. Wieler</i> .....	5187

Osbornite in CB/CH-like Carbonaceous Chondrite Isheyevo <i>V. I. Grokhovsky</i> .....	5231
In-situ Fe-XANES Study of Grains Trapped in Aerogel: An Analytical Test for the Interpretation of Stardust Samples Analyses <i>F. Grossemy, J. Borg, and A. Simionovici</i> .....	5276
A Spectacular Compound Chondrule-CAI in Northwest Africa 2918, a New CO3.1 Chondrite <i>J. N. Grossman, G. J. MacPherson, E. P. Vicenzi, and C. M. O'D. Alexander</i> .....	5283
Identification of Reidite from the Ries Impact Crater Using Micro-Raman Spectroscopy: A Review <i>A. Gucsik</i> .....	5103
The High-Energy View of Star Formation <i>M. Güdel</i> .....	5099
Water in Bencubbin <i>N. Guilhaumou, C. Fiéni, C. Perron, B. Ghasharova, and Y.-L. Mathis</i> .....	5223
Experiments on Chondrule Formation by “Lightning” <i>C. Güttler, T. Poppe, J. Blum, T. Springborn, and J. Wasson</i> .....	5124
Titanium Isotopic Ratios in KJG Presolar SiC Grains from Murchison <i>F. Gyngard, S. Amari, M. Jadhav, K. Marhas, E. Zinner, and R. S. Lewis</i> .....	5334
From Size Sorting of Chondrules to Accretion of Parent Bodies — The Effects of Photophoresis <i>H. Haack, O. Krauss, and G. Wurm</i> .....	5199
Mass-fractionation Induced by the Genesis Solar Wind Concentrator: Analysis of Neon Isotopes by UV Laser Ablation <i>V. S. Heber, R. C. Wiens, C. Olinger, D. S. Burnett, H. Baur, U. Wiechert, and R. Wieler</i> .....	5314
Rare Presolar Silicon Carbide Grains from Novae: An Automated Search by NanoSIMS <i>Ph. R. Heck, P. Hoppe, E. Gröner, K. K. Marhas, H. Baur, and R. Wieler</i> .....	5054
Solar Noble Gases in 470 Myr Old Fossil Micrometeorites <i>Ph. R. Heck, B. Schmitz, H. Baur, and R. Wieler</i> .....	5055
Dust in Protoplanetary Disks <i>Th. Henning</i> .....	5392
An Occurrence of Jarosite in MIL 03346: Implications for Conditions of Martian Aqueous Alteration <i>C. D. K. Herd</i> .....	5027
Some Methods to Systematically Document the Components of Chondrites <i>R. K. Herd, P. A. Hunt, and K. E. Venance</i> .....	5362
History of Metal Veins in Acapulcoite-Iodranite Clan Meteorite GRA 95209 <i>J. S. Herrin, D. W. Mittlefehldt, and M. Humayun</i> .....	5374
Laboratory Adsorbed Nitrogen and Noble Gases — Are We on the Safe Side? <i>S. Herrmann, S. P. Schwenger, and U. Ott</i> .....	5131

Bulk Composition of Chondrules in Carbonaceous Chondrites <i>D. C. Hezel, H. Palme, and R. Kießwetter</i> .....	5303
Neodymium, Samarium and Gadolinium Isotopic Studies of Lunar Meteorites Dhofar 489 and NWA 032 <i>H. Hidaka and S. Yoneda</i> .....	5169
A Possible Meteorite Lag Deposit After Continental Glaciation in Southeastern Manitoba <i>A. R. Hildebrand, M. Beech, S. A. Kissin, and G. B. Quade</i> .....	5378
Why Does Angra Dos Reis Have an Anomalous (Type B) NIR Spectrum? <i>E. J. Hoffman</i> .....	5319
New Finds of Shatter Cones in Distal Ries Ejecta, Bernhardzell, Eastern Switzerland <i>B. A. Hofmann and E. Gnos</i> .....	5127
The Twannberg, Switzerland IIG Iron: New Finds, CRE Ages and a Glacial Scenario <i>B. A. Hofmann, S. Lorenzetti, O. Eugster, F. Serefiddin, D. Hu, G. F. Herzog, and E. Gnos</i> .....	5128
Petrology and REE Geochemistry of the Lunar Meteorite Sayh Al Uhaymir 300 <i>W. Hsu, Y. Guan, T. Ushikubo, R. Bartoschewitz, A. Zhang, Th. Kurtz, and P. Kurtz</i> .....	5200
Sulfide Variations in CR Chondrites <i>H. Huber and A. E. Rubin</i> .....	5371
Layered Tektites and Adjacent Soils from SE Thailand <i>H. Huber and J. T. Wasson</i> .....	5370
Selenium and Sulphur Distribution in the Anomalous CK Chondrite EET 99430 <i>H. Huber, H. A. Ishii, and S. Brennan</i> .....	5324
The Exposure History of the Very Large L6 Chondrite JaH 073 <i>L. Huber, B. Hofmann, E. Gnos, and I. Leya</i> .....	5069
P-T Equilibration Conditions for Lunar Granulitic Impactites: Evidence from Apollo 15, 16, and 17 <i>J. A. Hudgins and J. G. Spray</i> .....	5256
Ni-rich Olivine and a CAI with Al-Diopside in NWA 2748, LL3.4 ± 0.2 <i>R. Hutchison and A. Kearsley</i> .....	5028
FIB-TEM and SIMS of Aeolian and Glacial Antarctic Micrometeorites — Evidence for Origin of “COPS” <i>K. A. Huwig and R. P. Harvey</i> .....	5291
A Transmission Electron Microscope Study of Internal Subgrains in SiC-X Grains <i>K. M. Hynes, T. K. Croat, S. Amari, A. F. Mertz, and T. J. Bernatowicz</i> .....	5333
Isotopic Analysis of the Sun <i>T. R. Ireland and M. Asplund</i> .....	5176
Oxygen Isotopes in Brachina, SAH 99555 and Northwest Africa 1054 <i>A. J. Irving and D. Rumble III</i> .....	5288

More African Enstatite-rich Meteorites: Aubrite NWA 2828, Zaklodzie-like NWA 4301, NWA 1840 and EL6 Chondrites <i>A. J. Irving, S. M. Kuehner, T. E. Bunch, J. H. Wittke, D. Rumble III, and G. M. Hupé</i> .....	5264
Global Catastrophic Changes on the Terrestrial Planets Caused by Large Impacts: An Implication to the Permafrost Formation on Mars <i>V. S. Isaev and K. A. Kondrat'eva</i> .....	5046
Unique Zoned Chondrules in the Isheyvo CH/CBb-like Chondrite and Their Aqueous Alteration <i>M. A. Ivanova and C. A. Lorenz</i> .....	5089
Concentric-zoned Inclusions in the Kaidun Meteorite <i>M. A. Ivanova, N. N. Kononkova, and A. V. Ivanov</i> .....	5090

## IRON AND NICKEL IN UREILITE SILICATES— CHEMISTRY AND ISOTOPES

A. Gabriel<sup>1\*</sup>, G. Quitté<sup>2</sup>, R. Schönberg<sup>1</sup>, J. Schübler<sup>1</sup> and A. Pack<sup>1</sup>, <sup>1</sup>Institut für Mineralogie, Universität Hannover, Callinstraße 3, D-30167 Hannover. <sup>2</sup>Institute of Isotope Geochemistry and Mineral Resources, ETH Zentrum, Clausiusstraße 25, CH-8092 Zürich. \*E-mail: a.gabriel@mineralogie.uni-hannover.de.

**Introduction:** Ureilites are ultramafic rocks comprising of olivine, low- and high-Ca pyroxene and C-rich material that occurs along grain boundaries [1]. Their formation is usually attributed to asteroidal differentiation [1], but a nebular setting has also been proposed [2].

**Results:** We have begun our study with ICP-OES (University of Hannover) trace element analyses (Fe, Co, Ni, Mn, Ca) of inclusion free silicate separates of the Kenna ureilite. We have estimated the *ol* composition (we have separated a mixture with ~13% *px* and ~87% *ol*) using the Fe/Ni *ol-opx*-partitioning data by [3] and FeO electron microprobe data to 18.8±0.3 wt.% FeO and 350±11 µg/g Ni (67±17 µg/g Co). Based on the *ol*-metal partitioning data by [4], our data suggest that metal coexisting with Kenna *ol* should contain ~20–60 wt.% Ni (2000 K > T > 1000 K). If we assume a chondritic Kenna parent asteroid (bulk) with ~20 wt.% FeO and negligible Ni in the mantle, the Fe,Ni core should contain only ~10 wt.% Ni. The discrepancy between the two approaches can be explained in terms of Fe/Ni distribution between ultramafic rocks (ureilites) and basalt *after* core separation during partial mantle melting or subsequent fractional crystallization.

The iron isotope composition of the Kenna silicates (MC-ICPMS, University of Hannover) is  $\delta^{56/54}\text{Fe} = +0.035 \pm 0.049\%$  ( $2\sigma$ ). Within uncertainty this value is indistinguishable to the mean of 14 bulk chondrite analyses ( $\delta^{56/54}\text{Fe} = -0.015 \pm 0.020\%$  [5]), the mean magmatic iron meteorite composition ( $\delta^{56/54}\text{Fe} = +0.047 \pm 0.016\%$ ;  $N = 8$  [5]) and the mean composition of non-cumulate and polymict eucrites ( $\delta^{56/54}\text{Fe} = -0.001 \pm 0.017\%$ ;  $N = 8$  [5]). More data will be provided to obtain information about the Fe-isotope composition of the reservoir from which ureilites formed and its relation to other achondrites.

The <sup>60</sup>Fe-<sup>60</sup>Ni short-lived isotope chronometer ( $t_{1/2} = 1.5$  Ma) is well suited to precisely date the formation of ureilites. Ni isotope analyses were conducted at ETH Zurich for an olivine fraction. Our *very preliminary* data suggest a <sup>60</sup>Ni excess of +0.5%. If true, this would correspond to an initial  $^{60}\text{Fe}/^{56}\text{Fe} \approx 3 \times 10^{-7}$  and a time interval of ~3 Ma after the start of the solar system (initial  $^{60}\text{Fe}/^{56}\text{Fe}$  taken from [6]). This is higher than  $^{60}\text{Fe}/^{56}\text{Fe} < 1.2 \times 10^{-7}$  as reported by [7].

We will obtain more data on different ureilites to discuss the chronological issue in more detail.

**References:** [1] Goodrich, C.A. (1992) *Meteor.* 27, 327. [2] Clayton, R.N. & T.K. Mayeda (1988) *GCA* 52, 1313. [3] Witt-Eickschen, G. & H.St.C. O'Neill (2005) *CG* 221, 65. [4] Seifert, S., *et al.* (1988) *GCA* 52, 603. [5] Schoenberg, R. & F. von Blanckenburg (2006) *EPSL* (submitted). [6] Mostefaoui, S., *et al.* (2004) *NAR* 48, 155. [7] Kita, N.T., *et al.* (1997) *LPSC XXVIII*, #1052.

**SPECTROSCOPY AND THE ASTEROID-METEORITE LINK: A PERSPECTIVE AFTER THREE DECADES**

M. J. Gaffey. Department of Space Studies, Odegard School of Aerospace Sciences, University of North Dakota, Grand Forks, North Dakota 58202-9008 USA. E-mail: [gaffey@space.edu](mailto:gaffey@space.edu)

**Introduction:** The “holy grail” of asteroid spectral studies has been to identify the specific parent bodies of the meteorites in order to place the detailed compositional, genetic and temporal data from meteorite studies into a spatial context in the early solar system. In the early 1970’s when asteroid spectroscopy was in its infancy, most of us naively assumed that the asteroid-meteorite linkages would quickly reveal themselves. The identification of asteroid 4 Vesta as the probable parent body of the HED meteorites encouraged this optimistic outlook. However, failures to quickly identify other probable meteorite parent bodies – and the failure of many of the early identifications to survive subsequent scrutiny - led to disillusionment for many in the asteroid spectroscopy community. Even three decades into the effort, the probable parent bodies of only four meteorite types (HEDs, H-chondrites, IIE irons, and aubrites - making up ~40% of all meteorite falls) have been identified.

**Meteoritics and Dynamics:** Steady progress has been made over the past two decades across a broad range of disciplines which allows a much more optimistic outlook for our future understanding of the asteroid-meteorite link. Advances in meteorite science have brought both subtlety and nuance to many of our simplistic early models of meteorite formation and relationships; models which govern much of our thinking about asteroids. Advances in the dynamical studies of asteroids have provided a better understanding of the evolution of the asteroid population, and of the mechanisms that deliver meteorites to the Earth. Dynamical studies have increased our understanding of the general linkages between asteroids and meteorites (such as the central importance of proper motion and secular resonances) while simultaneously challenging our ability to link meteorites to specific parent bodies (e.g., the Yarkovsky effect delivering meteoroids into resonances from relatively distant parent bodies).

**Advances in Asteroid Spectroscopy:** Our ability to obtain robust and sophisticated asteroid mineralogical characterizations suitable for comparison to meteoritic data has advanced ever more rapidly in the past two decades. The initial very limited techniques of curve matching have increasingly given way to the use of spectral parameters which are diagnostic of the presence, abundance and composition of a number of cosmically important mineral species. Combined with improvements in telescopic instrumentation, observing protocols, data reduction methodologies and interpretive calibrations the quality of asteroid mineralogical characterizations has increased dramatically. Space weathering - one of the great bugaboos of asteroid spectroscopy – has yielded to detailed study. While still not completely understood, the effects of space weathering can now be effectively eliminated in asteroid mineralogical characterizations.

**Conclusions:** We stand on the threshold of a golden age in our understanding of the origin and early evolution of the inner solar system from the asteroid-meteorite relationship. In addition to significantly enhancing our ability to identify plausible and probable meteorite parent bodies, the newer asteroid spectroscopic capabilities also provide information on bodies that are not represented in the meteorite collections enhancing our understanding of the late solar nebula and early solar system.

## PETROLOGY AND GEOCHEMISTRY OF THE NWA 3368 EUCRITE

K. G. Gardner<sup>1</sup>, D. S. Lauretta<sup>1</sup>, D. H. Hill<sup>1</sup>, J. S. Goreva<sup>1</sup>, K. J. Domanik<sup>1</sup>, I. A. Franchi<sup>2</sup>, and M. J. Drake<sup>1</sup>. <sup>1</sup>Lunar and Planetary Laboratory, University of Arizona. <sup>2</sup>Planetary and Space Sciences Research Institute, Open University. *kgardner@lpl.arizona.edu*

**Introduction:** A considerable amount of debate exists on the petrogenesis of eucrites, basaltic meteorites believed to have originated on 4 Vesta [1]. Many scientists have speculated on the formation event, supplementing ideas to Mason's fractional crystallization model and Stolper's partial melting model ([2-5]). Thus, an understanding of major and trace element compositions of all eucrites is imperative. Here, we report the petrology and trace element geochemistry of NWA 3368.

**Methods:** Two thin sections and one 20.5 gram polished slab were studied using a Cameca SX-50 electron microprobe. Six sub-samples including four clasts, a section of light-colored matrix, and a section of dark-colored matrix were extracted from the polished slab, and each piece was analyzed by both INAA and ICP-MS using the UA Nuclear Reactor Laboratory-LPL Gamma Ray Analysis Facility and the LPL ICP-MS facility, respectively [6]. A series of custom-made solutions of basaltic composition and the Geological Society of Japan standard basalt JB-2 were used as standards. Two small chips of NWA 3368 were sent to Open University to determine oxygen isotope composition.

**Results:** NWA 3368 has a variety of dark and light angular clasts that range in size from several millimeters to a couple of centimeters in length. They range in texture from coarse- to fine-grained. The fine-grained texture is composed of abundant plagioclase and lamellae-free pyroxene, while the coarse-grained texture contains abundant pyroxenes with varying degrees of exsolution lamellae. Electron microprobe analyses yielded pyroxene compositions of  $Wo_5En_{36}Fs_{59}$  for low-Ca pyroxene and  $Wo_{43}En_{30}Fs_{27}$  for high-Ca pyroxene. Plagioclase has a composition of  $An_{90}Ab_{10}Or_{0.4}$ . Ilmenite and troilite grains are abundant, along with chromite containing 5 to 27%  $TiO_2$  and ~5%  $Al_2O_3$ . Other phases include iron metal and silica. All Fe/Mn ratios lie between 28 and 32, typical for eucrites. Trace element data reveal a flat REE pattern with a slightly negative Eu anomaly. Sm vs. Sc, La, and Eu plots all reveal a pattern normal to eucrites. Similarly, O-isotope data are consistent with other HEDs [7].

**Conclusions:** NWA 3368 is a non-cumulate, monomict eucrite breccia related to known eucrites. The two separate lithologies, particularly the pyroxene exsolution, probably represent two separate thermal events that may be either metamorphic or primary igneous in origin. The REE abundances and patterns, as well as other trace element abundances, are typical of normal or main group eucrites.

**References:** [1] Consolmagno G. J. and Drake M. J. (1977) *Geochim. Cosmochim. Acta*, **41**, 1271-1282. [2] Stolper E. M. (1977) *Geochim. Cosmochim. Acta*, **41**, 587-611. [3] Mason B. (1962) *Meteorites*. 274 pp. [4] Ikeda Y. and Takeda H. (1985) *LPSC XV; JGR*, **90** (suppl), C649-C663. [5] Righter K. and Drake M. J. (1997) *M&PS*, **32**, 929-944. [6] Gardner K. G. et al. (2006) *Lunar and Planetary Science XXXVII*, #2389. [7] Mittlefehldt, D. W. et al. (1998) *Planetary Materials*, **36**, 4-103-130.

**Acknowledgements:** This work was supported by NASA grant NAG 12795 to M. J. Drake. Special thanks go to William Boynton for use of the LPL Gamma Ray Analysis Facility.

**COMPOSITION IN THE PROTOSOLAR AND LOCAL INTERSTELLAR CLOUDS—IMPLICATIONS FOR THE CHEMICAL EVOLUTION IN THE GALAXY DURING THE LAST 5 GYR.**

J. Geiss<sup>a</sup> and G. Gloeckler<sup>b</sup> <sup>a</sup>International Space Science Institute, Bern, Switzerland <sup>b</sup>Department of Atmospheric, Oceanic and Space Sciences, University of Michigan, Ann Arbor, USA

Our concepts of nucleosynthesis, as well as what we know about the origin of the elements and their isotopes are largely based on abundance measurements in the solar system. We know the relative abundance of nearly 300 nuclear species in the Protosolar Cloud (PSC), a sample of Galactic matter frozen-in (in terms of nuclear evolution) 4.6 Gyr ago. In meteorites, we also have measurements of isotopic ratios in stellar grains that were included in asteroids at the time of solar system formation. These grains have preserved the isotopic signature of matter released from stellar sources, such as AGB stars or supernovae.

Although we have a large body of spectroscopic composition data from galactic and extra-galactic objects, missing until recently was a sample of the present-day Galaxy with reliable observations of a number of elemental and isotopic abundance ratios, all measured in one and the same sample. Investigation of the composition in the Local Interstellar Cloud (LIC) is beginning to fill this gap.

Elemental and isotopic abundances in the LIC, obtained so far by in situ ion mass spectrometry, ACR measurements and remote spectroscopy will be summarized. Also, methods of deriving PSC abundances from solar wind composition measurements will be discussed.

By comparing abundances in the LIC and in the PSC we have investigated the Galactic evolution during the last 5 Gyr, using the mixing model introduced by Geiss, Gloeckler and Charbonnel (*ApJ*, **578**, 862, 2002). The effect of “infall” on the evolution of chemical and isotopic abundances in the Galaxy and the source of the infalling matter will be discussed.

**EQUILIBRATED ORDINARY CHONDRITE-LIKE MICROMETEORITES.**

M. J. Genge. Impact and Astromaterials Research Centre (IARC), Imperial College London and The Natural History Museum, Exhibition Road, London SW7 2AZ, UK. Email: m.genge@imperial.ac.uk

**Introduction:** Amongst unmelted micrometeorites (MMs) recovered from Antarctic ice are coarse-grained particles dominated by pyroxene, olivine and glass, that usually have igneous textures. On the basis of the mineral chemistries, textures and the presence of small amounts of fine-grained matrix Genge (1) has suggested these are mainly fragments of chondrules. Mineral chemistries, furthermore, suggest that ~70% of coarse-grained MMs are derived from ordinary chondrite-like parent bodies. The majority of such particles are unequilibrated, however, 7 particles (9%) have been reported that have olivine and pyroxene major and minor element compositions within the restricted range of the equilibrated ordinary chondrites (2).

In this study the chemistry, texture and mineralogy of equilibrated particles is examined to confirm their EOC origin.

**Samples and Methods:** The 7 equilibrated cgMMs were identified amongst a collection of 77 cgMMs collected from Antarctic ice. Selection and analytic techniques are described in Genge et al., (1).

**Results:** The EOC-like particles are dominated by olivine and pyroxene with homogeneous major and minor element compositions within the range of H and L4-6 chondrites. Five particles have granular textures and lack significant mesostasis. Accessory phases in the granular particles are taenite, albitic feldspar and Cr-spinel. Two particles have porphyritic textures and have vesicular mesostases dominated by pyroxene and olivine dendrites within aluminosilicate glass. One of these particles contains Ni-bearing sulphides in the mesostasis and one albitic feldspar. Both porphyritic particles have rounded particle shapes implying melting during atmospheric entry. One of the granular cgMMs also has a small area of compositionally variable vesicular glass containing partially melted feldspar.

**Discussion:** The reported particles have mineral compositions that are consistent with an EOC origin. The occurrence of albitic feldspar ( $An_{13-20}$ ) in combination with the olivine and pyroxene minor elements is in particular strong evidence for an EOC origin (3). Cr-bearing spinels are unfortunately too small for quantitative analysis.

The presence of glass within the mesostases of three of the particles, however, is not compatible with an EOC origin. The generation of compositionally variable, vesicular glass, often containing partially melted albitic glass, however, is observed in the thermally altered substrates of EOC fusion crusts (4). The formation of vesicles, presumably occurring due to degassing of sulphides under oxidizing conditions. Considering the evidence for surface correlated melting in these particles, the presence of mesostasis probably represents the overprint of entry heating.

Due to their small size it is difficult to apply petrologic grade criteria to MMs. Chromite-olivine geothermometry may offer a method by which this can be evaluated for selected particles.

**References:** [1] Genge M. J. et al., (2005) MAPS, 40, 255-238. [2] Genge M. J. (2006) LPSC, 37, #1759, [3] Brearley A. J. & Jones R. H. (1998) Planetary Materials. MSA, 36, 120-518. [4] Genge M. J. & Grady M. M. (1999) MAPS, 34, 341-356.

### STABLE IRON ISOTOPE ANALYSES OF METAL GRAINS IN ORDINARY CHONDRITES BY MC-ICP-MS.

K. J. Gildea<sup>1</sup>, R. Burgess<sup>1</sup>, I. Lyon<sup>1</sup> and D. W. Sears<sup>2</sup>. <sup>1</sup>School of Earth, Atmospheric and Environmental Sciences, The University of Manchester, Oxford Road, Manchester, M13 9PL, UK. [karen.j.gildea-1@student.manchester.ac.uk](mailto:karen.j.gildea-1@student.manchester.ac.uk). <sup>2</sup>Arkansas Center for Space and Planetary Science, University of Arkansas, Fayetteville, Arkansas 72701, USA.

**Introduction:** Stable iron isotope analyses of meteorites are being studied to help determine the processes involved in their formation, the source of their materials and subsequent surface alteration. Variation in iron isotope fractionation may be influenced by metal/silicate fractionation, metamorphism, aqueous alteration, chondrule formation and terrestrial weathering. The aim of this study is to assess whether the effects of these processes can be distinguished by analysing separated iron metal grains from 25 ordinary chondrites consisting of different classes (H, L and LL), different petrographic types (3-6) and different terrestrial weathering status (falls and finds).

**Equipment:** Analysis was by Nu Instruments multi-collector ICP-MS. Isobaric interferences were reduced by the introduction of samples via a DSN-100 Desolvating Nebuliser and by running the ICP in medium resolution mode to ensure that the Fe isotopes were sufficiently resolved to show a flat topped peak with 'iron shoulder' [1].

The reproducibility and accuracy of the ICP-MS was determined by measuring the 'in-house' Johnson-Matthey standard against the IRMM014 iron isotope standard using the sample/standard bracketing method to give  $\delta^{56}\text{Fe} = 0.33 \pm 0.06\%$  and  $\delta^{57}\text{Fe} = 0.5 \pm 0.07\%$  (to 1 standard deviation).

**Samples and sample preparation:** Samples were crushed and separated [2]. The magnetic separates were re-crushed and metal grains hand picked for  $\text{HNO}_3$  dissolution using a microscope.

#### Results:

	$\delta^{56}\text{Fe}$	s.e.	$\delta^{57}\text{Fe}$	s.e.
Bremervörde (H3)	-0.01	0.04	-0.02	0.05
Beaver Creek (H4)	0.08	0.04	0.12	0.08
Elm Creek (H4)	0.13	0.02	0.26	0.02
Acme (H5)	0.19	0.05	0.27	0.06
Crumlin (L5)	0.19	0.02	0.36	0.06
Etter (L5)	0.19	0.02	0.36	0.02
Aldsworth (LL5)	0.24	0.04	0.42	0.04
Barwell (L6)	0.33	0.02	0.55	0.08

When plotted these results trend along a mass fractionation line with  $\delta^{56}\text{Fe}$  and  $\delta^{57}\text{Fe}$  increasing with petrographic order. Further results will be presented at the meeting along with discussion and conclusion.

**Acknowledgements:** This work was supported by PPARC and by the University of Manchester through SRIF funding for the Nu Plasma MC-ICP-MS.

**References:** [1] Weyer S. & Schweiters J. B. 2003. *Int. J. of Mass Spec.* 226:355-368. [2] Sears D. W. & Axon H. J. 1976. *Nature* 260:34-35.

**IRON OXIDATION STATE IN AUSTRALASIAN MICRO-TEKTITES BY HIGH-RESOLUTION XANES SPECTROSCOPY AND  $K_{\beta}$ -DETECTED XANES SPECTROSCOPY**

Gabriele Giuli<sup>1\*</sup>, Sigrid Griet Eeckhout<sup>2</sup>, Christian Koeberl<sup>3</sup>, Eleonora Paris<sup>1</sup>, Giovanni Pratesi<sup>4,5</sup>. <sup>1</sup> Dip. Scienze della Terra, Università di Camerino, Italy; gabriele.giuli@unicam.it. <sup>2</sup> European Synchrotron Radiation Facility (ESRF), Grenoble, France. <sup>3</sup> Dept. of Geological Sciences, University of Vienna, Austria. <sup>4</sup> Museo di Storia Naturale, Università di Firenze, Italy.

We examined the iron oxidation state and coordination number in 6 micro-tektites from the Australasian strewn field by a combination of high-resolution X-ray Absorption Near Edge Structure (XANES) and X-ray Emission spectroscopy (XES). The latter technique ( $K_{\beta}$ -detected XANES spectroscopy) has the advantage of displaying sharper peaks in the pre-edge region, thus allowing a better resolution and a more straightforward way of decomposing the pre-edge features into its components. The spectra have been collected at ID26 beamline of the ESRF storage ring (Grenoble, France). The X-ray beam (size = 30 x 80  $\mu\text{m}$ ) has been monochromatised with two Si (220) crystals. XANES and XES spectra consistently show small variations in the energy and intensity of the pre-edge peaks. Comparison with Fe model compounds with known Fe oxidation state and coordination number allowed us to estimate the Fe oxidation state for the micro-tektites under study.

Within experimental reproducibility, all the pre-edge peak energies of the micro-tektite samples plot very close to the divalent Fe model compounds.  $\text{Fe}^{3+}/(\text{Fe}^{2+} + \text{Fe}^{3+})$  are estimated to be in the 0 to 0.1 range.

Comparison with literature data on splash form tektites from all four known strewn field [1] and impact glass from a K/T boundary layer [2] allows us to confirm that, as for the Fe oxidation state, Australasian micro-tektites are indistinguishable from splash form tektites. On the other hand, noticeable differences are observed with K/T impact glasses, which in the view of these data should not be considered as micro-tektites.

**References:** [1] Giuli G. et al. 2002. *Geochimica et Cosmochimica Acta*, 66:4347-4353. [2] Giuli G. et al. 2005. *Meteoritics and Planetary Science*, 40:1575-1580.

**IRON OXIDATION STATE IN IMPACT GLASS FROM THE CRETACEOUS/TERTIARY BOUNDARY AT BELOC (HAITI) BY HIGH-RESOLUTION XANES SPECTROSCOPY: IMPLICATIONS ON THE FORMATION CONDITIONS.**

Gabriele Giuli<sup>1\*</sup>, Sigrid Griet Eeckhout<sup>2</sup>, Christian Koeberl<sup>3</sup>, Giovanni Pratesi<sup>4,5</sup>, Eleonora Paris<sup>1</sup>. <sup>1</sup>Dip. Scienze della Terra, Università di Camerino, Italy; gabriele.giuli@unicam.it. <sup>2</sup>European Synchrotron Radiation Facility (ESRF), Grenoble, France. <sup>3</sup>Dept. of Geological Sciences, University of Vienna, Austria. <sup>4</sup>Museo di Storia Naturale, Università di Firenze, Italy.

We examined the iron oxidation state and coordination number in five yellow impact glasses from the Cretaceous-Tertiary (K/T) boundary section at Beloc, Haiti, which formed as the result of impact melting during the Chicxulub impact event. The samples have been analyzed by Fe K-edge high-resolution X-ray Absorption Near Edge Structure (XANES) spectroscopy, and the resulting data on Fe oxidation state and coordination number have been compared with literature data on 9 black impact glasses and 1 High Si-K impact spherule from the same impact layer.

Although there are several studies on the chemical and isotopic composition of these impact glasses, very few studies on the Fe coordination number and oxidation state have been reported [1]. Such studies are, however, of utmost importance to reconstruct the oxygen fugacity conditions prevailing during impact melt formation.

The Fe K-edge high-resolution X-ray Absorption Near Edge Structure (XANES) spectra have been recorded at the ID26 beamline of the ESRF storage ring (Grenoble, F). The pre-edge peaks of our XANES spectra display noticeable variations in intensity and energy, which are indicative of significant changes in the Fe oxidation state, spanning a wide range from about 20 to 100 mole% trivalent Fe. All data plot along a trend, falling between two mixing lines joining a point calculated as the mean of a group of tektites studied so far (consisting of 4- and 5- coordinated Fe<sup>2+</sup>) to <sup>[4]</sup>Fe<sup>3+</sup> and <sup>[5]</sup>Fe<sup>3+</sup>, respectively. Thus, the XANES spectra can be interpreted as a mixture of <sup>[4]</sup>Fe<sup>2+</sup>, <sup>[5]</sup>Fe<sup>2+</sup>, <sup>[4]</sup>Fe<sup>3+</sup> and <sup>[5]</sup>Fe<sup>3+</sup>. There is no evidence for six-fold coordinated Fe, however, its presence in small amounts cannot be excluded from XANES data alone. Yellow glasses display clearly higher Fe<sup>3+</sup>/(Fe<sup>2+</sup> + Fe<sup>3+</sup>) ratios (from 75 to 100 mole % trivalent Fe [3]) when compared to black impact glasses (from 20 to 75 mole % trivalent Fe [2]) and high Si-K glass (20 mole % trivalent Fe). Our observations are explained by a very large variety of oxygen fugacity conditions prevailing during melt formation. Furthermore, there is a clear positive relationship between the Fe<sup>3+</sup>/(Fe<sup>2+</sup> + Fe<sup>3+</sup>) ratio and the Ca content of the studied glasses, suggesting that the Fe oxidation state was affected by a variable contribution of the Ca-sulphate bearing sedimentary rocks overlying the target rock at the impact site.

**References:** [1] Oskarsson N. et al. 1996. In: Ryder G., Fastovsky D. and Gartner S. (eds.) *New Developments Regarding the KT Event and Other Catastrophes in Earth History*. Geological Society of America, Special Paper 307, pp 445-452. [2] Giuli G. et al. 2005. *Meteoritics and Planetary Science*, 40:1575-1580. [3] Giuli G. et al. (2007) in prep.

**DIVALENT VANADIUM IN VIGARANO CV3 METEORITE CHONDRULE.**

Gabriele Giuli<sup>1\*</sup>, Giovanni Pratesi<sup>2</sup>, Sigrid Griet Eeckhout<sup>3</sup>, Eleonora Paris<sup>1</sup>, <sup>1</sup> Dip. Scienze della Terra, Università di Camerino, Italy; [gabriele.giuli@unicam.it](mailto:gabriele.giuli@unicam.it). <sup>2</sup> Museo di Storia Naturale, Università di Firenze, Italy. <sup>3</sup> European Synchrotron Radiation Facility (ESRF), Grenoble, France.

A chondrule of the CV3 Vigarano carbonaceous chondrite has been studied by high-resolution XANES spectroscopy in order to get accurate information on the V oxidation state. Comparison of the experimental spectrum with those of V model compounds with known oxidation state and coordination number provided strong evidence of the presence of divalent vanadium in the chondrule examined.

In the aim of establishing the location of V in the minerals making up the chondrule, experimental spectra have been calculated for a set of mineral structures possibly hosting vanadium. For each mineral, theoretical spectra have been calculated and this for each crystallographic site possibly hosting V, and the results have been summed with different weights in order to better reproduce the experimental spectrum.

Comparison with the experimental spectrum rules out preferential incorporation of V in magnetite, whereas forsterite, enstatite and diopside can all be accounted for as possible hosts for V.

The presence of divalent vanadium in a chondrule of a CV3 chondrite has never been reported in the literature, and bear important consequences on the formation conditions of this class of meteorites.

**THE JaH 091 STREWNFIELD**

E. Gnos<sup>1</sup>, M. Eggimann<sup>2</sup>, A. Al-Kathiri<sup>3</sup> and B. A. Hofmann<sup>2</sup>.  
<sup>1</sup>Institut für Geologie, Universität Bern, Baltzerstrasse 1, 3012 Bern, Switzerland. E-mail: gnos@geo.unibe.ch.  
<sup>2</sup>Naturhistorisches Museum der Burgergemeinde Bern, Bernstrasse 15, 3005 Bern, Switzerland. <sup>3</sup>Directorate General of Commerce and Industry, Ministry of Commerce and Industry, Salalah, Sultanate of Oman

**Introduction:** Initial finds of two paired large masses of an L5 meteorite in 2002 (JaH 090, 92.7 kg; JaH 091, 123.7 kg; ~5.7 km distance between the two localities) suggested the presence of a large meteorite strewnfield in Oman. Additional stones recovered in 2003 yielded the orientation of the strewnfield. We were able to extend the strewnfield length to >40 km in spring 2005, and additional systematic searches for larger masses so far yielded ~2300 kg of material. Searches at the smaller mass end of the strewnfield confirmed the field over a length of 49 km x 9 km making it one of the largest meteorite strewnfields known, comparable to Jilin and Allende. JaH 091 is moderately weathered (W2-W3), its shock grade is S2 and mineral compositions are  $\text{Fa}_{25.0} \text{Fs}_{21.3} \text{Wo}_{1.6}$ . The material characteristically shows half to >1cm sized olivine chondrules at its surface. Larger stones commonly show small holes on its lower side in the soil.

**Relations with JaH 055:** As the published JaH 055 (L4-5) coordinate fell in the area of another well-searched strewnfield (JaH 073) we were amazed to learn that we should have missed such a large mass. Further searches around the published coordinates and in our JaH 073 collection confirmed the absence of any L4-5 stones such as JaH 055. Meteorites seized by the Omani police from illegal meteorite collectors in 2005 were labeled JaH 055 and associated coordinates were close to JaH 091. This material is >700 kg and includes large fragments. The finding of similar large masses within the JaH 091 strewnfield sparked the idea that an error in the published coordinate could solve the discrepancy. From the finders of JaH 055 we were informed that the JaH 055 coordinate is indeed in error, and we thus think that JaH 091 and JaH 055 are in fact paired. This would bring the total mass known to ~3200 kg.

**Possible connection to locality name:** It is interesting to note that according to a Bedouin legend an area near the JaH 091 strewnfield is called "LAHOOB" meaning "Big Fire". Qualitative age estimates using weathering grade and other weathering proxies [2] indicate that the JaH 091 fall occurred <15000 years ago. This may well be within humans tradition. The <sup>14</sup>C age of JaH 091 (19.3 ± 1.3 kyr [2]) may be strongly influenced by shielding.

**References:**

- [1] Russell S. et al. 2004. *Meteoritics & Planetary Science* 39:A215-A272. [2] Al-Kathiri A. et al. 2005. *Meteoritics & Planetary Science* 40:1215-1239.

**THE KREEP-RICH IMBRIUM IMPACT MELT BRECCIA OF THE LUNAR METEORITE SAYH AL UHAYMIR 169**

E. Gnos<sup>1</sup>, B. A. Hofmann<sup>4</sup>, A. Al-Kathiri<sup>3</sup> and M. J. Whitehouse<sup>4</sup>.

<sup>1</sup>Institut für Geologie, Universität Bern, Baltzerstrasse 3, 3012 Bern, Switzerland. E-mail: gnos@geo.unibe.ch.

<sup>2</sup>Naturhistorisches Museum der Burgergemeinde Bern, Bernastrasse 15, 3005 Bern, Switzerland <sup>3</sup>Directorate General of

Commerce and Industry, Ministry of Commerce and Industry, Salalah, Sultanate of Oman. <sup>4</sup>Laboratory for isotope geology, Swedish Museum of Natural History, Box 50007, SE-104 05, Stockholm, Sweden

**Introduction:** The dominant lithology (87 vol%) of the unique lunar meteorite Sayh al Uhaymir (SaU) 169 from Oman consists of an extremely KREEP-rich polymict, crystalline impact-melt breccia interpreted to be derived from the Imbrium impact melt sheet [1]. This lithology is now assigned together with few mm-sized rock fragments from the Apollo 12 and 14 landing sites to a grouplet called “high-Th impact melt group” [2].

**Results and interpretation:** The impact melt contains 25 - 40 vol% of shocked plutonic (gabbro-noritic to noritic) Procellarum-Terrane clasts characterized by the absence of anorthosites. Many plagioclase clasts show a high albite content reaching An<sub>57</sub>. The crystalline impact melt between the clasts consists mainly of low-Ca pyroxene, plagioclase intergrown with Ba-bearing K-spar, and smaller amounts of merrillite, zircon, olivine, troilite and kamacite. The SaU 169 impact melt bulk composition shows a strong enrichment in Th (32.7 µg/g), U (8.6 µg/g), K<sub>2</sub>O (0.54 wt%), REE (~1330 µg/g), P<sub>2</sub>O<sub>5</sub> (1.14 wt%), and Zr (2835 µg/g) [1]. LREE-enriched merrillite is the main REE carrier containing 4-9 wt% REE oxides. Zircon is characterized by HREE-enriched patterns with a negative Eu anomaly. Application of Ti-thermometer for zircon [3] yielded a minimum crystallization temperature of 1168 ± 33°C. SaU 169 impact melt ilmenites are characterized by containing ~0.6 wt% Nb<sub>2</sub>O<sub>5</sub>. The detailed analysis of all phases crystallized from the impact melt, in combination with its modal abundance and calculated mineral densities allows to estimate the “pure clast-free Imbrium KREEP melt” composed of: ~2.0 wt% P<sub>2</sub>O<sub>5</sub>, 44.4 SiO<sub>2</sub>, 4.9 TiO<sub>2</sub>, 10.9 Al<sub>2</sub>O<sub>3</sub>, 14.0 FeO, 12.2 MgO, 7.4 CaO, 0.8 Na<sub>2</sub>O, 0.4 K<sub>2</sub>O, ~380 Nb, ~1250 Ba, and ~3400 REEs. This indicates that highly evolved differentiates were present at the Imbrium impact site.

**References:** [1] Gnos E. et al. 2004. *Science* 305: 657–659. [2] Zeigler R. A. 2006. Abstract #2366. 37th Lunar & Planetary Science Conference. [3] Watson, E.B. and Harrison, T. M. 2005. *Science* 308:841–844.

## EFFECTS OF FALLING IMPACT EJECTA ON THE POST-CHICXULUB ATMOSPHERE

T. J. Goldin<sup>1,3</sup> and H. J. Melosh<sup>2,3</sup>. <sup>1</sup>Dept. of Geosciences, University of Arizona, Tucson, Arizona 85721. E-mail: tgoldin@geo.arizona.edu. <sup>2</sup>Lunar and Planetary Lab, University of Arizona, Tucson, Arizona 85721. <sup>3</sup>Bayerisches Geoinstitut D-95440 Bayreuth, Germany.

**Introduction:** The mechanics of impact ejecta deposition are not well understood, especially for planets with atmospheres, where complex interactions occur between the ejected particles and the surrounding atmosphere. Studying the interactions between the ejecta from large terrestrial impacts and the atmosphere is particularly important for understanding the environmental effects of such events.

The K/T boundary ejecta layer, linked to the 65-Ma Chicxulub impact, is found world-wide. This study focuses on the 2-3-mm thick [1] distal ejecta, which consists of densely packed spherules 250- $\mu$ m in average diameter [2]. Additionally, a global soot layer has been identified at the K/T boundary [3], suggesting the impact triggered global wildfires.

**Modeling:** KFIX-LPL is a version of the KFIX code [4], which has been modified to suit the problem of impact sedimentation. KFIX is based on the original KACHINA code [5]. The finite-difference code models two-dimensional, two-phase fluid flow allowing us to examine the interactions between the atmosphere and ejected spherules.

We modeled a simplified Chicxulub scenario with the injection of uniform 250- $\mu$ m diameter spherules into the atmosphere at 8 km/s, at an altitude of 200 km and with a variable inflow density consistent with the volume of spherules observed and models of mass deposition rates [6]. The initial mesh approximates the Earth's atmosphere. Air is modeled as a perfect gas and the spherules are modeled as a simple incompressible fluid with the properties of basaltic glass. We modeled both a vertical injection angle and a more realistic angle of 45 degrees. The particles fall through the thin upper atmosphere, pushing the atmosphere downwards until the particles decelerate due to drag and increasing atmospheric pressure. The particles accumulate at ~100-km altitude and the deceleration heats the atmosphere around the particles (>2500 K), causing expansion of the atmosphere and creating a sharp transition between hot dense atmosphere below the deceleration boundary and cool thin atmosphere above.

**Discussion:** These models provide important insight into the state of the atmosphere after the Chicxulub impact. It has been proposed that thermal energy radiated from ejecta reentering the atmosphere caused global wildfires [6] and our models provide support for significant atmospheric heating and thus the delivery of significant thermal radiation to the Earth's surface. Additionally, our results provide the starting conditions and timeframes for chemical models examining the environmental consequences of Chicxulub, such as acid rain and sulfate aerosol formation.

**References:** [1] Smit J. et al. 1992. *Proceedings of the Lunar and Planetary Science Conference* 22:87-100. [2] Smit J. 1999. *Annual Review of Earth and Planetary Science* 27:75-113. [3] Wolbach W. et al. 1985. *Science* 208:1095-1108. [4] Rivard W. C. and Torrey M. D. 1977. *Los Alamos National Laboratory Report* LA-NUREG-6623, Los Alamos, 125 pp. [5] Amsden A. A. and Harlow F. H. 1974. *Los Alamos Scientific Laboratory Report* LA-5680, Los Alamos. [6] Melosh H. J. et al. 1990. *Nature* 343:251-253.

## CONSTRAINING VOLATILE ABUNDANCE IN CHONDRITIC COMPONENTS.

S. H. Gordon<sup>1,2</sup>, P. A. Bland<sup>1,2</sup>, S. J. Hammond<sup>1,3</sup>, N. W. Rogers<sup>3</sup>.  
<sup>1</sup>Impact & Astromaterials Research Centre (IARC), Imperial College London, South Kensington Campus, London SW7 2AZ, UK. E-mail: s.h.gordon@imperial.ac.uk. <sup>2</sup>Department of Mineralogy, The Natural History Museum, Cromwell Road, London, SW7 5BD, UK. <sup>3</sup>Department of Earth Sciences, The Open University, Walton Hall, Milton Keynes MK7 6AA, UK.

**Introduction:** Volatile depletion was the fundamental chemical process occurring in the early Solar System, but has yet to be fully explained. Proposed models include the two-component model (e.g.[1,2]), incomplete condensation (e.g.[3,4]), evaporative fractionation prior to chondrule formation [5] and inheritance of a depletion from the interstellar medium [6]. These hypotheses are largely based on bulk compositional data from chondrites. A knowledge of the variation in composition of chondritic components (e.g. matrix and chondrules) may provide some useful constraints on the mechanism for volatile depletion.

In addition, an improved knowledge of their trace and minor element composition may help to clarify chondrule:matrix complementarity. Some models (e.g. [2]) call for chondrule formation close to the young Sun, with chondrules being added to chemically unrelated matrix at asteroidal distances. Complementarity between chondrules and matrix in siderophile and chalcophile elements (e.g.[7,8]) casts doubt on this scenario.

The relatively sparse data for many elements in chondrules and matrix is related to the difficulty in acquiring precise separates. The current study is intended to overcome this obstacle.

**Method:** Modal recombination analysis (MRA) [9] and electron probe microanalysis (EPMA) are used to determine the bulk composition of individual chondrules. A micromill is then used to drill precise volumes of material from a pre-specified area. Solution and LA-ICP-MS is subsequently employed to determine the chemistry of these separates. The ICP-MS data are then combined with major element data determined by MRA and EMPA.

**Results:** CV3 chondrites Allende and Vigarano were investigated initially, as chondrules are large and easily defined. In addition, Allende is one of the few meteorites for which chondrule minor and trace element data are available [10]. Data gained via MRA and EPMA fall within the compositional parameters defined in the literature. Solution ICP-MS will allow for the determination of a wider range of minor and trace elements than in previous INAA studies.

**Conclusions:** Matrix and chondrules have been analysed to investigate the extent of chemical complementarity between these two components, and to constrain mechanisms for volatile depletion. Results will be presented at the meeting.

**References:** [1] Anders E. 1964. *Space Sci. Rev.* 3:583. [2] Shu F.H. et al. 1996. *Science* 271:1545. [3] Wasson J.T. & Chou C-L. 1974. *Meteorit* 9:69. [4] Cassen P. 1996. *MAPS* 31:793. [5] Huss G.R. et al. 2003. *GCA* 67:4283. [6] Yin Q. 2005. *Chondrites and the Protoplanetary Disk*. 632. [7] Bland P.A. et al. 2005. *PNAS* 102:13755. [8] Kong P. & Palme H. 1999. *GCA* 63:3673. [9] Berlin J. et al. 2006. Abstract #2370. *LPSC XXXVII*. [10] Rubin A.E & Wasson J.T. 1988. *GCA* 52:425.

**Li-Be ISOTOPE SYSTEMATIC IN EFREMOVKA CAIs.**

J. N. Goswami and M. P. Deomurari, Physical Research Laboratory, Ahmedabad – 380009, India. (goswami@prl.res.in).

The presence of excess  $^{10}\text{B}$  from in-situ decay of  $^{10}\text{Be}$  (half-life = 1.5 Ma) in CAIs is well established [1-4]. Energetic particle interactions as well as  $^{10}\text{Be}$  of galactic cosmic ray origin, trapped within the protosolar cloud, are considered as potential sources of this nuclide in the early solar system [1-5]. A hint for the presence of the short-lived nuclide  $^7\text{Be}$  (half-life = 53 days) at the time of formation in an Allende CAI (3529-41) has been claimed recently [6]. Disturbance in the Al-Mg isotope system in this CAI is well documented [7] and an attempt was made to avoid this problem by accepting Li-Be isotope data for only those analyses where Be concentration was compatible with the expected fractionation trend during magmatic differentiation of CAI melt [6]. Presence of  $^7\text{Be}$  in early solar system, if confirmed, will uniquely identify local production of this nuclide via interactions of energetic particles from the early Sun. We have initiated a study of Efremovka CAIs to look for possible presence of  $^7\text{Li}$  at the time of their formation. Petrographic characteristics and Al-Mg isotope systematics do not suggest presence of any post-magmatic perturbation in almost all Efremovka CAIs [8]

We have analyzed melilite in the Efremovka CAIs E-2 and E-40 for Li-Be isotope records using a Cameca ims-4f ion microprobe. Both these CAIs have well behaved Al-Mg isotope systematics with initial  $^{26}\text{Al}/^{27}\text{Al}$  ratios of  $(5.64 \pm 0.97) \times 10^{-5}$  and  $(3.4 \pm 1.0) \times 10^{-5}$ , respectively [8, 9]. The isotopic studies were carried out at a mass resolution ( $M/\Delta M$ ) of  $\sim 1500$ , sufficient to remove all the molecular interferences at the masses of interest. We use GB-4 glass as a standard to correct for instrument mass fractionation as well as to infer the relative ion yields and absolute concentration of Li, Be and B in the analyzed phases. Our study confirms the dependence of Li ion yield, relative to Be, as a function of energy of the secondary ions accepted for analysis [6]. Li concentrations in the analyzed melilite from E-2 are  $\leq 0.06$  ppm, while Be contents are  $\leq 0.2$  ppm.

The results obtained so far do not provide any indication for the presence of resolved excess of  $^7\text{Li}$  in E-2 melilite. Further, the inferred initial  $^7\text{Li}/^6\text{Li}$  at the time of formation of E-2 is lower than the reference value. We note that multiple sources are needed for explaining the natural abundance of  $^7\text{Li}$  [10]. Thus, the lower initial  $^7\text{Li}/^6\text{Li}$  in the early formed refractory phases may imply heterogeneity in Li isotopic composition within the protosolar cloud that did not undergo complete mixing and homogenization by the time of CAI formation. We made a similar suggestion to explain variations in the initial boron isotopic composition in CAIs [11].

**References:** [1] McKeegan K. D. et al. 2000. *Science* 289: 1334-1337. [2] Sugiura N. et al. 2001. *MAPS* 36:1397-1408. [3] MacPherson G. J. et al. 2003. *GCA* 67:3165-3179. [4] Marhas K. K. et al. 2002. *Science* 298:2182-2185. [5] Desch S. J. et al. 2004. *Astrophys. J.* 602:528-542. [6] Chaussidon M. et al. 2006. *GCA* 70: 224-245. [7] Podosek F. A. et al. 1991. *GCA* 55 :1083-1110. [8] Goswami J. N. et al. 1994. *GCA* 58:431-447. [9] Fahey et al. 1987. *GCA* 51:3215-3229. [10] Walker T. P. et al. 1985. *Astrophys. J.* 299:745-751 [11] Goswami J. N. 2003. *MAPS* 38:A48.

**A  $^{16}\text{O}$ -RICH CAI-LIKE PARTICLE AMONG ANTARCTIC MICROMETEORITES.** M. Gounelle<sup>1,2,3</sup>, M. Chaussidon<sup>4</sup>, C. Engrand<sup>3</sup>, J. Duprat<sup>3</sup> and H. Leroux<sup>5</sup>. <sup>1</sup>LEME-MNHN, CP52, 57 rue Cuvier, 75005 Paris, France ([gounelle@mnhn.fr](mailto:gounelle@mnhn.fr)). <sup>2</sup>IARC, NHM London SW7 5BD, UK. <sup>3</sup>CSNSM, Bât. 104, 91405 Orsay Campus, France. <sup>4</sup>CRPG-CNRS, BP20, 54501 Vandoeuvre les Nancy, France. <sup>5</sup>LSPEs, 59655 Villeneuve d'Ascq, France.

**Introduction:** Antarctic micrometeorites (AMMs) are interplanetary dust particles collected in the Antarctic ice cap, and belonging to the size range 25-400  $\mu\text{m}$  [1]. They might represent the bulk of extraterrestrial matter accreting Earth today [2]. They bear strong resemblances with low petrographic type, hydrous carbonaceous chondrites [1]. Compared to IDPs they lack chondritic porous particles [3]. Antarctic micrometeorites might be of cometary or asteroidal origin, or a mixture thereof. Given the discovery of Calcium-, Aluminium-rich (CAI) particles among the Stardust samples [4], we have characterized a CAI-like particle among the AMMs collection.

**Results:** Micrometeorite 98-03-04 was collected at the Astrolabe glacier during the field season 1997-1998 [5]. After extraction under a binocular microscope, it was embedded in epoxy and polished. SEM examination has revealed an elongated, 100  $\mu\text{m}$  across, compact particle with some holes, probably due to loss of grains. It is made of diopside ( $\text{En}_{53-60}\text{Wo}_{39-50}$ ), spinel and other Ca-Al-rich minerals too small to be analyzed with the electron microprobe, all set up in a phosphorus-rich chondritic matrix and surrounded by a partial magnetite rim. Pyrrhotite is present at the boundary of the Ca-Al-rich minerals and the chondritic matrix. In a previous polishing plan, olivine ( $\text{Fo}_{68-97}$ ) was also found. The bulk oxygen isotopic composition, measured at the CRPG Nancy with the CAMECA 1270 ion probe, and expressed relative to the Standard Mean Ocean Water, is  $\delta^{17}\text{O} = -36.6 \pm 0.1 \text{‰}$ ,  $\delta^{18}\text{O} = -32.3 \pm 0.4 \text{‰}$ , i.e.  $\Delta^{17}\text{O} = -19.9 \pm 0.5 \text{‰}$ .

**Discussion:** The compact nature and mineralogy of micrometeorite 98-03-04 sets it apart from others CAI-like micrometeorites which are usually made of spinel ( $\pm$  perovskite) and iron-rich phyllosilicates [6, 7], or of isolated spinel and hibonite [8]. Though it lacks anorthite, it is reminiscent of the CAI particle found among Stardust samples. The oxygen isotopic composition of 98-03-04 is similar to other CAIs among Antarctic micrometeorites [6, 7, 9] or in carbonaceous chondrites [10], suggesting the existence of one common reservoir for all CAIs, possibly close to the Sun [11]. In this context, it will be of uttermost importance to measure the oxygen isotopic composition of CAI-like particles among Stardust samples.

**References:** [1] C. Engrand and M. Maurette, *MAPS* 33 (1998) 565-580. [2] J. Duprat, et al., *MAPS*, this volume (2006). [3] M. Gounelle, et al., *MAPS* 40 (2005) 917-932. [4] M.E. Zolensky, et al., *LPSC* 37 (2006) #1203. [5] M. Gounelle, et al., *MAPS* 34 (Supp) (1999) A46. [6] P. Hoppe, et al., *LPSC* 26 (1995) 623-624. [7] G. Kurat, et al., *MAPS* 29 (1994) 487-488. [8] M. Gounelle, PhD thesis, Université Paris 7, 2000. [9] C. Engrand, et al., *GCA* 63 (1999) 2623-2636. [10] R.N. Clayton, *Ann. Rev. Earth Planet. Sci.* 21 (1993) 115-149. [11] F.H. Shu, et al., *ApJ* 548 (2001) 1029-1050.

**DEPTH-DEPENDENT FRACTIONATION OF LIGHT SOLAR WIND NOBLE GASES IN A GENESIS TARGET.**

A. Grimberg<sup>1</sup>, F. Bühler<sup>2</sup>, P. Bochsler<sup>2</sup>, D.S. Burnett<sup>3</sup>, H. Baur<sup>1</sup> and R. Wieler<sup>1</sup>. <sup>1</sup>Isotope Geology, ETH Zürich. E-mail: grimberg@erdw.ethz.ch. <sup>2</sup>Physikalisches Institut, University of Bern. <sup>3</sup>GPS, CalTech, Pasadena.

We analyzed light noble gases in a bulk metallic glass (BMG) that was exposed to solar wind (SW) irradiation on Genesis for its total exposure time and all SW regimes [1]. The BMG was especially designed to look for a putative Solar Energetic Particle (SEP) component, reported to be present in lunar soils [2], by using the closed system stepwise etching (CSSE) technique. Here we present the depth distribution of He and Ne isotopes and discuss different processes leading to the observed fractionation patterns. Moreover, this will be compared with measurements of Ar isotopes that are actually in progress.

The Ne isotope depth distribution measured in the BMG resembles a fractionation pattern that follows a mass dependant fractionation line. Lighter isotopes are enriched at shallow depth with initial <sup>20</sup>Ne/<sup>22</sup>Ne higher than the bulk SW value, whereas the heavier isotopes are enriched in deeper layers. This distribution is fully consistent with model calculations using the SRIM code [3] of an isotopically uniform SW that fractionates within the BMG upon implantation, assuming a velocity distribution as measured by Genesis. From this it follows that there is no evidence for a distinct isotopic fractionation of Ne among the different SW regimes. Most importantly, the use of BMG data in combination with SRIM simulations, which allow for surface sputtering and cosmogenic Ne production in lunar grains, shows that no "SEP-Ne" component, that would be isotopically heavier than the SW-Ne, is needed to explain the lunar soil data.

The measured He isotopic distribution in the BMG is very different from the Ne fractionation pattern and also from the He distribution as simulated with SRIM for the same SW conditions applied for Ne. The <sup>3</sup>He/<sup>4</sup>He ratios released from shallow depth first increase by 10 % and later drop to almost constant values 13 % lower than the initial in all remaining steps. This is in contrast to SRIM simulations that predict a steep decrease of <sup>3</sup>He/<sup>4</sup>He with depth by more than a factor of 6. A diffusional loss, which in turn would have led to a smearing of the He isotope distribution, is unlikely. Bulk analyses show no difference of the He abundance compared to other Genesis targets [4] or in-situ spacecraft measurements. On the other hand it is well conceivable that the SRIM code overestimates the fractionation with depth for very light elements as He. However, the largely different isotope pattern between He and Ne suggests that the trapped solar He suffered an additional fractionation process not yet identified.

**References:** [1] Grimberg, A. et al. 2006. *Lunar Planet. Sci. Conf. XXXVII*, #1782. [2] Wieler R. et al. 1986. *Geochim. Cosmochim. Acta* 50: 1997-2017. [3] Ziegler J.F. 2004. *Nucl. Instr. Meth. Phys. Research* 219/220: 1027-1036. [4] Hohenberg, C.M. et al. 2006. *Lunar Planet. Sci. Conf. XXXVII*, #2439.

### OSBORNITE IN CB/CH-LIKE CARBONACEOUS CHONDRITE ISHEYEVO

V.I. Grokhovsky. Physico-Technical Department, Ural State Technical University – UPI, Ekaterinburg 620002, Russian Federation. E-mail: [grokh47@mail.ru](mailto:grokh47@mail.ru).

**Introduction:** Recently discovered metal-rich primitive meteorite Isheyevu genetically links CH and CB of carbonaceous chondrites [1]. As with other meteorites of the CR clan, the unique mineralogical and textural data of Isheyevu are being widely discussed [1-4]. Both nebular and asteroidal models have been proposed to explain this data [6]. Here we report the first discovery of the osbornite refractory mineral for the CR clan in Isheyevu chondrite.

**Results and discussion:** Optically, SEM/EDX and element X-ray mapping detected the large (~100  $\mu\text{m}$ ) grain of osbornite TiN in the area of CB-lithology by the so-called border between CB and CH chondrite in Isheyevu. Single crystal of osbornite (fig.1.) with Ti, N stoichiometric contents contacts both metal and silicates (olivine, pyroxene). The phase boundaries of these minerals are marked by thin secondary minerals. The osbornite possesses characteristic yellow color and is subject to low roughening in course of sample preparation.

TiN is a very refractory mineral. It is condensed at high temperatures under highly reducing conditions. Rare grains of osbornite occur in few EH and EL chondrites and aubrites. Besides that, TiN was found in ALH 85085 reduced carbonaceous chondrite [5] and, recently, the osbornite inclusion was observed in CAIs from Isheyevu [6]. It is concluded that there is no simple equilibrium process, which can explain all peculiarities of texture in Isheyevu meteorite, but it is clear that observed osbornite was among the first crystals formed from gaseous phase in the solar nebula.

**References:** [1] Ivanova M.A. et al; 2006. *LPSC XXXVII*, #1100. [2] Krot A.N. et al; 2006. *LPSC XXXVII*, #1224. [3] Perron C. et al; 2004. *AMSM 67*: #5041. [4] Righter K. et al; 2003. *LPSC XXXIV*, #1373. [5] Bischoff A. et al; 1993. *GCA 57*, 2631-2648. [6] Krot A.N. 2006. private communication.

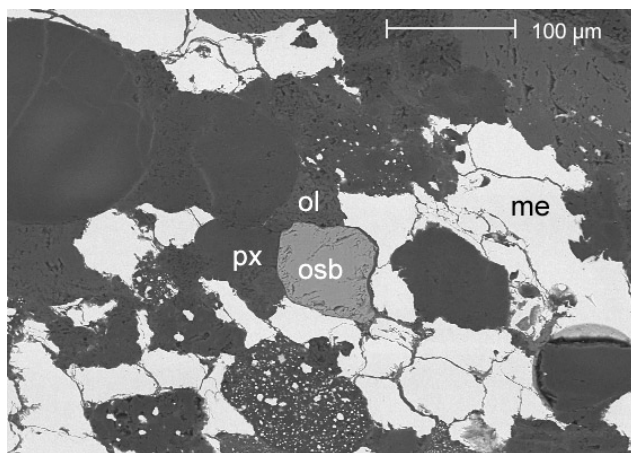


Fig.1. BSE image of the osbornite from Isheyevu. osb = osbornite TiN; me = Fe(Ni)-metal; px = pyroxene; ol = olivine.

**IN-SITU Fe-XANES STUDY OF GRAINS TRAPPED IN AEROGEL: AN ANALYTICAL TEST FOR THE INTERPRETATION OF STARDUST SAMPLES ANALYSES.**

F. Grossemy<sup>1</sup>, J. Borg<sup>1</sup> and A. Simionovici<sup>2</sup>. <sup>1</sup>Institut d'Astrophysique Spatiale, CNRS, Univ. Paris-Sud, UMR8617, Orsay Cedex, F-91405. E-mail: faustine.grossemy@ias.u-psud.fr. <sup>2</sup>Laboratoire des Sciences de la Terre, ENS Lyon, France.

**Introduction:** In January 2006, the Stardust mission of the NASA brought back to Earth aerogel collectors in which grains of the comet Wild-2 as well as interstellar grains have been trapped [1]. Here we report on an experiment carried out to study the slowing down of hypervelocity particles into aerogel. Micrometer-sized grains trapped inside pieces of aerogel, a few hundreds of microns large, were analysed. They originate either from the Orbital Debris Collection Experiment (ODCE) of the NASA exposed outside the Mir station from 1997 to 1998, or from gas gun shots in Stardust's aerogel of grains from the Allende meteorite. Micro-fluorescence mappings and XANES spectra at the iron K-edge have been performed on these samples using the X-ray Microscopy beamline ID21 at the ESRF, Grenoble (France).

**Results:** From the micro-fluorescence mappings, both the trapped grain and its penetration track were identified. It can be concluded from the Fe "hot spots" found along the track that the incident grain broke up into many fragments while entering and slowing down in the aerogel in spite of its very low density.

XANES spectra at the Fe K edge were then acquired in hot-spot regions. For each spectrum, the energy of the absorption edge and the centroid energy of the pre-edge were used to determine the Fe redox states, following [2]. The edge and the pre-edge centroid are indicative of an evolution from a Fe<sup>3+</sup> form at the track entrance to a more reduced form along the track and in the final grain. Beam-induced photo-reduction was checked for by acquiring several spectra on the same points and seeing no shift towards lower energies.

**Discussions:** Given the observed Fe redox state of the particles in the aerogel, several mechanisms can be inferred. Based on the results for the Allende sample, known to be Fe<sup>2+</sup> rich [3, 4], the most probable one is the following. Incident grains of 2+ oxidation state undergo rapid oxidation to 3+ at the entrance of the track, due to high temperature slowing down from the initial velocity of a few km.s<sup>-1</sup> in the presence of the aerogel oxygen. The shell of oxidized iron is lost at the track entrance by the grain that remains in the 2+ oxidation state at the end of the track. This suggests that the final grain has the same mineralogy as the incident one, which is crucial for current and upcoming Stardust analyses.

**References:** [1] Tsou P. et al. 2006. 37th Lunar and Planetary Science Conference. 2189. [2] Wilke M. et al. 2001. *American Mineralogist* 86:714–730. [3] Olivier F.W. et al. 1984. *Meteoritics & Planetary Science* 19, 1, 25-27. [4] Hoffman E. et al. 2000. *Meteoritics & Planetary Science* 35, 2, 431-434.

### A SPECTACULAR COMPOUND CHONDRULE-CAI IN NORTHWEST AFRICA 2918, A NEW CO3.1 CHONDRITE.

J. N. Grossman<sup>1</sup>, G. J. MacPherson<sup>2</sup>, E. P. Vicenzi<sup>2</sup> and C. M. O'D. Alexander<sup>3</sup>. <sup>1</sup>U. S. Geological Survey, Reston, VA 20192, USA. E-mail: jgrossman@usgs.gov. <sup>2</sup>Dept. Mineral Sciences, Smithsonian Institution, Washington, DC 20560-0119. <sup>3</sup>Carnegie Institution of Washington, Washington, DC 20015-1305

**Introduction:** Northwest Africa (NWA) 2918 was recently classified as a very primitive, type 3.0, CO chondrite [1]. Our analysis of the Cr content of ferroan olivine using the method of [2] shows a distribution very similar to that in DOM 03238 [3], lacking a prominent mode near 0.4 wt% Cr<sub>2</sub>O<sub>3</sub> as in type 3.0; mean Cr<sub>2</sub>O<sub>3</sub> = 0.24 ± 0.12 wt%. Both meteorites are probably type 3.1 and have experienced very light thermal metamorphism.

Optical examination of a 2-cm<sup>2</sup> thin section of NWA 2918 revealed a typical CO chondrite texture, with an abundance of small chondrules and Ca-Al-rich inclusions (CAIs). A deep-blue, circular object 170 μm in diameter was conspicuous in transmitted light. This object is a CAI partially enveloped by a type I, porphyritic pyroxene (PP) chondrule. Compound objects consisting of CAIs and ferromagnesian chondrules are extremely rare [4], and this one has many unusual properties worthy of study.

**Mineralogy/petrology:** The chondrule portion of the compound object is unremarkable in mineralogy. Low-Ca pyroxenes, Fs<sub>1.5</sub>Wo<sub>1.5</sub> are richer in refractory elements than is normal for PP chondrules (2.4% Al<sub>2</sub>O<sub>3</sub>, 0.4% TiO<sub>2</sub>), and poikilitically enclose olivine (Fa<sub>2</sub>). Abundant oxidized grains, formerly rich in Fe metal are present. Mesostasis is anorthite or anorthitic glass, richest in TiO<sub>2</sub> near the CAI and Na<sub>2</sub>O away from it. Ca-rich pyroxene is also abundant.

The core of the CAI is dominantly a deep-blue colored spinel that has 2.0 wt% TiO<sub>2</sub>, 0.6 wt% Cr<sub>2</sub>O<sub>3</sub> and 0.6 wt% FeO. Spinel near the rim of the CAI has 1.3 wt% TiO<sub>2</sub> and is nearly colorless. A pale-blue spinel grain previously extracted from Murchison [5] was not rich in TiO<sub>2</sub>. The outer portion of the CAI is mostly anorthite or anorthitic glass. Like the spinel, anorthite is high in TiO<sub>2</sub> near the CAI core (0.4 wt%) and has ~half as much near the rim. Several crystals of an unidentified Ti-rich oxide phase occur in the CAI core, with 85% TiO<sub>2</sub>, 10% MgO and 4% Al<sub>2</sub>O<sub>3</sub>. Nepheline and Ca-rich pyroxene are present in the outer part of the CAI, but only on the surface away from the chondrule. Tiny metal grains rich in Fe, Ru and Mo are also present in the CAI.

**Discussion:** This compound object formed by the collision of an unusual Ti-rich CAI with a molten or partially molten chondrule. The absence of perovskite is puzzling; there is no evidence that the Ti-rich oxide is secondary after perovskite. The chondrule minerals experienced chemical exchange with those in the CAI, leading to zoning and refractory enrichment. Entry of alkalis occurred after the compound object solidified, resulting in sodic plagioclase in the chondrule far from the CAI and nepheline in the CAI far from the chondrule. Isotopic studies are underway to determine the chronology of the events leading to the formation of the object as well as the origin and nature of the minerals in the strange CAI.

**References:** [1] Connolly H. C. Jr. et al. 2006. *M&PS* 41:in press, [2] Grossman J. N. and Brearley A. J. 2005. *M&PS* 40:87-122. [3] Grossman J. N. and Rubin A. E. 2006. Abstract #1383. 27th LPSC. [4] Krot A. N. et al. 2006. *Ap. J.* 639: 1227-1237. [5] MacPherson et al. 1983. *GCA* 47:823-839.

## IDENTIFICATION OF REIDITE FROM THE RIES IMPACT CRATER USING MICRO-RAMAN SPECTROSCOPY: A REVIEW

A. Gucsik<sup>1</sup>. <sup>1</sup>University of West Hungary, Bajcsy-Zs. u. 4., Sopron, Hungary. E-mail: ciklamensopron@yahoo.com

**Introduction:** The phase transformation from the zircon crystal structure ( $ZrSiO_4$ ) to a scheelite ( $CaWO_4$ )-structure phase (reidite) was described in shock-metamorphosed zircon by Kusaba et al. [1] to begin at about 30 GPa and to be complete at around 53 GPa. These observations were confirmed by Leroux et al. [2] through their TEM investigations of experimentally shocked zircon. More recently, according to Scott et al. [3] the high-pressure x-ray data show that a small amount of residual zircon-structured material remained at 39.5 GPa. Glass et al. [4] found the scheelite-type phase in zircon samples from marine sediments from an upper Eocene impact ejecta layer sampled near New Jersey and Barbados. They named this mineral phase 'reidite' after Alan F. Reid, who first produced this high shock-pressure polymorph of zircon [4]. The purpose of this investigation is to further investigate the capability of the Raman spectroscopy to document shock deformation and to determine whether specific Raman effects in zircon/scheelite-structure can be utilised to determine particular shock pressure stages.

**Experimental Procedure:** Raman spectra were obtained on shocked single zircon grains from the Ries impact structure with a Renishaw RM1000 confocal micro-Raman spectrometer with a 20 mW, 632 nm He-Ne laser excitation system and a thermoelectrically cooled CCD detector. The power of laser beam on sample was approximately 3 mW. Spectra were obtained in the range 100-1200  $cm^{-1}$  with approximately thirty seconds total exposure time. The spectral resolution (apparatus function) was 4  $cm^{-1}$ .

**Results and Discussion:** The Raman spectra of the naturally shock-deformed zircon samples from the Ries Crater (Stage-II: 35-45 GPa, Stage-III: 45-50 GPa, Stage-IV: >50 GPa) cut parallel and perpendicular to their crystallographic c-axis do not exhibit significant differences from each other. Stage-II samples are characterized by five peaks at 224, 356, 439, 974 and 1007  $cm^{-1}$ . Addition Raman spectrum of the Stage-III (45-50 GPa) sample (parallel) shows eleven peaks at 202, 224, 327, 356, 404, 439, 465, 558, 845, 974 and 1007  $cm^{-1}$ , which indicate the presence of the scheelite-type phase among predominant zircon-type material. In general, the fluorescence background in the parallel-sample is considerably higher than in the perpendicular-sample. In both cases, the peak intensities are similar. The spectra of the Stage-IV samples (parallel- and perpendicular-samples) are characterized by seven peaks at 202, 215, 225, 356, 439, 974 and 1007  $cm^{-1}$ .

**Conclusion:** Raman spectroscopy is a potentially useful tool that can be used to characterize the shock stages of zircon from impactites. These results also give new insight into the structural changes that occur in zircons during shock metamorphism, and the pressures associated with these changes.

**Acknowledgement:** This work has been partly supported by Hungarian Space Office (TP-293)

**References:** [1] Kusaba K. et al. (1985) *Earth Planet. Sci. Lett.* 72: 433-439. [2] Leroux H. et al. (1999) *Earth Planet. Sci. Lett.* 169: 291-301. [3] Scott H.P. et al. (2002) *Physical Rev. Lett.* 88: 015506-1-015506-4. [4] Glass B.P. et al. (2002) *American Mineralogist* 87: 562-565.

**THE HIGH-ENERGY VIEW OF STAR FORMATION.**

M. Güdel<sup>1</sup>. <sup>1</sup>Paul Scherrer Institut, Würenlingen and Villigen, CH-5232 Villigen PSI, Switzerland. E-mail: guedel@astro.phys.ethz.ch.

Although stars form in very cold, molecular environments, observations with X-ray satellites reveal stellar environments rich in high-energy radiation (X-rays). X-ray luminosities up to four orders of magnitude above solar levels are common in protostars and T Tau stars. Most of this emission is thought to originate from heated plasma trapped in a corona or magnetosphere around the stars, although alternative X-ray generation mechanisms have been proposed, such as shock-heating in accretion columns [1] or shocks in outflows and jets [2,3]. It is likely that X-ray emission is, like in the case of the Sun, accompanied by high-energy particle streams ejected in particular during magnetic energy release events. Non-thermal radio emission has indeed provided spectacular evidence for the presence of relativistic electrons around some systems.

High-energy radiation and particle beams have a profound impact on the stellar environment, in particular on circumstellar disks in which planets eventually form. They heat disk surfaces, partly ionize the disk gas, and induce chemistry at various locations in the stellar environment (e.g., [4]).

Furthermore, high-energy, ionizing radiation is important in the process of planet formation and the buildup of planetary atmospheres. This may be of particular relevance to our understanding of the early evolution of the inner planets in our solar system [5].

This presentation will summarize selected aspects of high-energy emission and magnetic fields around young, forming stars, addressing i) the origin and characteristics of high-energy radiation and particles around forming stars, ii) the role of magnetic fields around young stars, iii) the potential impact of high-energy radiation (+particles) on the stellar environment, and iv) evidence for a violent environment of the young Sun.

**References:** [1] Kastner J. H. et al. 2002. *Astrophysical Journal* 567:434. [2] Bally J. et al. 2003. *Astrophysical Journal* 584:843. [3] Güdel M. et al. 2005. *Astrophysical Journal* 626:L53. [4] Glassgold A. E. et al. 2004. *Astrophysical Journal* 615:972. [5] Ribas I. et al. 2005. *Astrophysical Journal* 622:680.

**WATER IN BENCUBBIN.**

N. Guilhaumou<sup>1</sup>, C. Fiéni<sup>1</sup>, C. Perron<sup>1</sup>, B. Ghasharova<sup>2</sup> and Y.-L. Mathis<sup>2</sup>. <sup>1</sup>Museum National d'Histoire Naturelle, 75005 Paris, France. [guilhau@mnhn.fr](mailto:guilhau@mnhn.fr). <sup>2</sup>Institute for Synchrotron Radiation, 76021 Karlsruhe, Germany.

**Introduction:** The origin of Bencubbin and its few siblings (hereafter CB chondrites) is still controversial, and we have no clear explanation for some of their most intriguing properties. CB chondrites have suffered at least one shock event in their parent-body, as testified by the metal-silicate melt that fills all spaces between large grains. In Bencubbin, vesicles containing <sup>15</sup>N-rich nitrogen gas were found in glassy phases [1,2]. We have extended this work, and find that water also is present in the vesicles, in the phases in which these are set, and in the impact melt.

**Experimental:** Self-supporting, doubly-polished sections, 70-140 μm thick, were prepared in anhydrous conditions from the MNHN Bencubbin specimen. They were studied by micro-infrared spectroscopy, using the synchrotron source at the ANKA facility, Karlsruhe. The phases studied include the silicate portion of the impact melt and phases in which bubbles were observed, namely the mesostasis in large silicate grains and the chondrule mesostasis in an ordinary chondrite (OC) inclusion.

**Results:** Water was detected in bubbles both in the mesostasis in the host and in the chondrule mesostasis in the OC inclusion, by means of the two bands of the bending and stretching modes of molecular H<sub>2</sub>O, respectively centered at 1634 and 3567 cm<sup>-1</sup>. It was also detected in the two bubble-bearing mesostases themselves, and in the silicate portion of the impact melt. Slight differences in the shape and position of the band of the stretching mode, and maps of IR absorbance in the range 3200-3600 cm<sup>-1</sup> allowed us to distinguish water vapor in the bubbles from water in the glassy phases.

The water content of the glasses was estimated by comparison with glasses of known water contents. It varies from 2500 to 4500 ppm, with no significant differences between the different phases studied. The main uncertainty on these values results from the uncertainty on the thickness of the studied phases, taken as one half that of the thin section. In the host mesostasis bubbles are present only in some parts. In the parts with no bubbles that we studied, water was below detection limit (i.e. <100 ppm).

**Discussion:** Our interpretation is that water (and <sup>15</sup>N-rich nitrogen) was degassed during a shock event in the Bencubbin parent-body. At the same time, in addition to the impact melt, some phases with low melting temperatures (mesostasis in the host, mesostasis of chondrules in the OC inclusion) were also partially melted, at least in the part of Bencubbin we studied. Water (and N<sub>2</sub>) dissolved in the liquids, then partially degassed when pressure and temperature decreased, leading to the formation of vesicles. Where did water come from? Hydrated matrix lumps have been observed in some CB chondrites, and in the related CH chondrites [3]. It has been suggested that this sort of material was the precursor of the impact melt [4]. Our findings support this hypothesis, and suggest that this hydrated matrix was initially abundant in Bencubbin.

**References:** [1] Marty B. et al. 2000. Abstract #1489. 31<sup>st</sup> Lunar & Planetary Science Conference. [2] Perron C. et al. 2001. *Meteoritics & Planetary Science* 36:A160. [3] Greshake A. et al. 2002. *Meteoritics & Planetary Science* 37:281. [4] Meibom A. et al. 2005. *Meteoritics & Planetary Science* 40:1377.

**EXPERIMENTS ON CHONDRULE FORMATION BY “LIGHTNING”**C. Güttler<sup>1</sup>, T. Poppe<sup>1</sup>, J. Blum<sup>1</sup>, T. Springborn<sup>1</sup> and J. Wasson<sup>2</sup>.<sup>1</sup>Institut für Geophysik und extraterrestrische Physik, Technische Universität Braunschweig, Mendelssohnstr. 3, 38106 Braunschweig, Germany. E-mail: C.Guettler@TU-Braunschweig.de.<sup>2</sup>Institute for Geophysics and Planetary Physics, University of California, 405 Hilgrad Avenue, Los Angeles, CA 90095-1567 USA

**Introduction:** Chondrules are generally assumed to have formed in the early solar system from macroscopic dust agglomerates largely composed of micrometer-sized grains. One among other hypotheses on the heating mechanism is that electrical discharges in the solar nebula transformed the dust into melt spherules. There is one single experiment reported [1] in which ground meteoritic material was exposed to a 5 kJ discharge. Most material was dispersed, some spherules up to 200  $\mu\text{m}$  in diameter were found, which, unlike meteoritic chondrules, were porous.

We are presently conducting an experimental study to tackle the question whether and under which conditions a discharge can transform a sample of micrometer-sized grains into chondrule-like spherules. Thus we exposed samples of silica, iron, fayalite, albite and peridot agglomerates of micrometer-sized dust grains to a 500 J electric discharge between two electrodes of 3 mm distance. The ambient air pressure was between 0.1 mbar and atmospheric pressure. The objects are analyzed by optical microscopy and with scanning electron microscopy.

**First Results:** Largely independent of the nature of the sample and the gas pressure, the dust was instantly dispersed by the discharge, but a small part was thermally processed. Together with unprocessed dust we found different types of large objects, among them spherules, depending on the material: Iron built many hollow spheres of all sizes up to 300  $\mu\text{m}$  in diameter whereas fayalite formed only a few spherules of about 50  $\mu\text{m}$  in diameter and clusters of sizes up to 200  $\mu\text{m}$  consisting of crystals and original grains. Similar clusters were also found with albite, peridot and silica precursors, which formed no spherules. A few typical spherules were embedded in epoxy resin for sectioning. Under the microscope they revealed bubbles to a varying extent (fayalite) or were even completely hollow (iron). The fraction of material converted into spherules was in general extremely low. Assuming that 2 kJ/kg is necessary for melting [2], the energetic efficiency (energy for melting/electrical energy) of lightning heating is less than  $10^{-5}$ .

**Summary:** We transformed dust agglomerates of micrometer-sized grains into spherules containing molten material by a gas discharge. The spherules are quite small, although some are of chondrule size. However in contrast to chondrules, the spherules had bubbles or even were hollow. Also, the energetic efficiency of our discharge heating is extremely low. Extrapolating to solar nebular conditions, chondrule formation by lightning is inconsistent with any reasonable assumptions on the energy of possible nebular lightning strokes, although it is an open issue whether the energetic efficiency might be higher under different conditions, e.g., a different linear scale.

**References:** [1] Wdowiak T. J. 1983. In *Chondrules and their origins*. p. 279-283. [2] Wasson J.T. 1996, In *Chondrules and the protoplanetary disk*. p. 45-54.

### TITANIUM ISOTOPIC RATIOS IN KJG PRESOLAR SiC GRAINS FROM MURCHISON.

F. Gyngard<sup>1</sup>, S. Amari<sup>1</sup>, M. Jadhav<sup>1</sup>, K. Marhas<sup>1</sup>, E. Zinner<sup>1</sup>, and R. S. Lewis<sup>2</sup>, Laboratory for Space Sciences and Department of Physics, Washington University, St. Louis, MO 63130, USA, [fmgyngar@wustl.edu](mailto:fmgyngar@wustl.edu), <sup>2</sup>Enrico Fermi Institute, University of Chicago, Chicago, IL 60637, USA.

**Introduction:** Thousands of individual presolar SiC grains have been measured for their C and Si isotopic compositions [1-3]. Despite the fact that Ti is one of the most abundant trace elements in SiC, only approximately 110 SiC grains have had their Ti isotopic compositions determined [1,4-7], but most analyses suffer from selection effects. Specifically, the Ti data for mainstream SiC, thought to have formed in the outflows of low-mass (1–3M<sub>⊙</sub>) C-rich Asymptotic Giant Branch (AGB) stars [8], have not been obtained from a representative sample of the larger population. The grains analyzed have been chosen either for their high Ti concentrations [4] or their large <sup>29</sup>Si and <sup>30</sup>Si excesses [1]. To rectify this situation, we report here the Ti isotopic composition of 75 of the 247 SiC grains we have randomly selected for these measurements.

**Experimental:** Energy Dispersive X-ray (EDX) analysis was performed on grains from a Murchison KJG separate (diameter 2–4.5 μm) [9] dispersed on gold foil. After identification as SiC, 247 grains of size roughly ≥ 2.5 μm were randomly selected for isotopic measurement in the Washington University NanoSIMS, with this lower limit on grain size in place only to ensure suitably precise Ti results. Carbon, N, and Si isotopic ratios were measured first and the Ti isotopes for 75 of the grains measured afterwards by a combination of peak jumping and multidetection. Signals from <sup>44</sup>Ca, <sup>51</sup>V, <sup>52</sup>Cr, and <sup>53</sup>Cr were also monitored in order to correct for Ca interferences at masses 46 and 48 and Cr and V interferences at mass 50.

**Results:** The  $\delta^{46,47,49,50}\text{Ti}/^{48}\text{Ti}$  values measured cover a range comparable to what has been seen previously [1,4], and plot along correlation lines in Ti 3-isotope plots. The data also exhibit a linear correlation between Si and Ti isotopic ratios, similar to what has been previously observed, indicative of a Galactic chemical evolution component in the grains' Si and Ti compositions [10-12]. Hoppe et al. [1] observed that Ti in SiC is usually characterized by enrichments in the minor isotopes relative to <sup>48</sup>Ti, resulting in a V-shaped pattern; here, we have found that roughly 40% of the grains measured so far exhibit this pattern, while about 55% have irregular patterns and the rest (5%) have an inverted pattern. The grains of this study can be grouped into three broad categories based on the Ti concentration as a function of depth: those with very negligible amounts of Ti, virtually at the limit of sensitivity (~10%); those with relatively uniform Ti concentration (~40%); and those with marked variation - often orders of magnitude changes - in Ti concentration, likely due to the presence of Ti subgrains (~50%).

**References:** [1] Hoppe P. et al. 1994. *ApJ* 430: 870-890. [2] Hoppe P. et al 1996. *GCA* 60:883-907. [3] Nittler L. R. and Alexander C. M. O'D. 2003. *GCA* 67:4961-4980. [4] Alexander C. M. O'D. and Nittler L. R. 1999. *ApJ* 519:222-235. [5] Amari S. et al. 2001. *ApJ* 546:463-483. [6] Amari S. et al. 2001. *ApJ* 559:248-266. [7] Zinner E. et al. 2005. *LPS XXXVI*, Abstract #1691. [8] Hoppe P. and Ott U. 1997. In *Astrophysical Implications of the Laboratory Study of Presolar Material* pp. 27-58. AIP, New York. [9] Amari S. et al. 1994. *GCA* 58:459-470. [10] Lugaro M. et al. 1999. *ApJ* 527:369-394. [11] Lugaro M. and Gallino R. 2001. *MAPS* 36:A118. [12] Nittler L. R. 2005. *ApJ* 618:281-296.

## FROM SIZE SORTING OF CHONDRULES TO ACCRETION OF PARENT BODIES – THE EFFECTS OF PHOTOPHORESIS

H. Haack<sup>1</sup>, O. Krauss<sup>2</sup>, and G. Wurm<sup>2</sup>. <sup>1</sup>Natural History Museum of Denmark, Øster Voldgade 5-7, DK-1350 Copenhagen K, Denmark. E-mail: hh@snm.ku.dk. <sup>2</sup>Institute for Planetology, Wilhelm-Klemm-Str 10, D48149 Münster, Germany.

**Introduction:** Recent evidence based on <sup>26</sup>Al chronology suggest that the differentiated asteroids accreted ~0.7 My after CAI formation, while chondrules were still forming in the nebula [1]. Chondrules appear to have been size-sorted prior to accretion [2] suggesting that physical processes allowed rapid accretion of some asteroids while components of other asteroids formed and were being size-sorted at the same time. Observations of asteroids and theoretical models suggest that the differentiated asteroids formed closer to the Sun than primitive asteroids, possibly in the terrestrial planet forming region [3]. We believe that several of these observations could be attributed to photophoresis, which have recently been shown to be of significance while gas and dust coexisted in the Solar nebula [4].

**Chondrule and CAI based constraints:** Several clues to the sorting and concentration processes come from the observations of chondrules and CAIs in chondrites. 1) Chondrules are better sorted than CAIs [5]. If the sorting process was operating on a small scale we should expect that all of the locally available components were equally well sorted. We thus infer that the sorting process was operating on a large scale. 2) Chondrules are common in all types of equilibrated chondrites whereas CAIs are only common in carbonaceous chondrites, 3) CAIs apparently formed close to the Sun but are mainly found in carbonaceous chondrites believed to originate in the outer part of the asteroid belt. 4) Differences in oxygen isotope signatures show that the source regions for ordinary, enstatite, and carbonaceous chondrites were separated from each other in space and/or time.

**Photophoresis and size sorting in the nebula:** We suggest that photophoresis could have two significant effects on the particle motion in the Solar nebula. In the early stages while the nebula was still optically thick photophoresis would help concentrate particles at the inner edge of the disk leading to enhanced accretion rates here [6]. As the nebula became optically thin photophoresis pushed chondrules and CAIs out to the point where inward motion caused by gas drag is balanced by the outward motion caused by photophoresis and radiation pressure. The particles will drift toward the radial distance where the forces balance and since the photophoresis is a size dependent force, different size ranges of chondrules and CAIs will accumulate and subsequently accrete at different heliocentric distances. As the gas gets thinner and thinner the accumulation point will move inward [7]. The first chondritic bodies will therefore accrete in the outer parts of the belt and probably include the majority of the remaining CAIs. As the accumulation point moves inward, later generations of chondrules will be incorporated in chondrite parent bodies largely devoid of CAIs, in the inner part of the asteroid belt.

**References:** [1] Bizzarro M. et al. 2005, *Astrophysical Journal*, 632, L41-L44. [2] Kuebler K.E. et al. 1999, *Icarus* 141, 96-106. [3] Bottke W.F. et al. 2006, *Nature* 439, 821-824. [4] Wurm G. and Krauss O. 2006. *Icarus*, 180, 487-495. [5] May C. et al. 1999. Abstract #1688. 30th Lunar & Planetary Science Conference. [6] Wurm G. et al. This issue. [7] Petit J.-M. et al. 2006. Abstract #1558. 37th Lunar & Planetary Science Conference.

**MASS-FRACTIONATION INDUCED BY THE GENESIS SOLAR WIND CONCENTRATOR: ANALYSIS OF NEON ISOTOPES BY UV LASER ABLATION.**

V. S. Heber<sup>1</sup>, R. C. Wiens<sup>2</sup>, C. Olinger<sup>2</sup>, D. S. Burnett<sup>3</sup>, H. Baur<sup>1</sup>, U. Wiechert<sup>4</sup>, R. Wieler<sup>1</sup>; <sup>1</sup>Isotope Geology, NW C85, ETH, CH-8092 Zürich Switzerland, heber@erdw.ethz.ch; <sup>2</sup>LANL, Space & Atmospheric Sci., Los Alamos, NM 87544, USA; <sup>3</sup>CalTech, JPL, Pasadena, CA 91109 USA; <sup>4</sup>AG Geochemie, FU Berlin, 12249 Berlin, Germany.

The solar wind (SW) concentrator, a key instrument onboard the Genesis Mission, was designed to provide larger fluences of implanted SW for precise isotope analyses of oxygen and nitrogen [1]. SW ions in the mass range 4 - 28 amu were accelerated and focussed onto a "concentrator target" by an electrostatic mirror. This concentration process caused some instrumental mass fractionation of the implanted SW ions as function of the radial position on the target. Correction of this fractionation will be based on a combination of the measured radial fractionation of Ne isotopes with results of simulations of the implantation process using the actual performance of the concentrator and the SW conditions during exposure. Here we present He and Ne abundance and Ne isotopic composition data along one arm of the gold cross that framed the 4 concentrator sub-targets.

He and Ne were released from pits ~120  $\mu$ m in diameter by UV laser ablation using a 248 nm Eximer laser [2]. In the first 34 analyses He and Ne were analysed together at constant analytical conditions. In a second set of 16 analyses, He and Ne were separated to protect the mass spectrometer from solar <sup>3</sup>He. In total, 12 positions along the arm (30 mm long) were analysed, each with 1 to 6 single analyses. He and Ne abundances increase from the edge (at 30 mm) towards the centre of the concentrator cross, He from 5.3E+15 ions/cm<sup>2</sup> (at 20.5 mm) to 1.8E+16 ions/cm<sup>2</sup> (at 2.9 mm) and Ne from 3.5E+12 ions/cm<sup>2</sup> (at 29.4 mm) to 3.4E+13 ions/cm<sup>2</sup> (at 1 mm). Thus, the concentration factor increases by about a factor of 10, similar to expected values from post-flight models for oxygen. Applying a simplified backscatter correction measured and expected Ne abundances agree within 20%. The measured Ne isotopes show a large mass fractionation as function of the target radius. The <sup>22</sup>Ne values (relative to SW <sup>20</sup>Ne/<sup>22</sup>Ne of 13.75, [3]) range from -19‰ (at 26 mm) to +40‰ (at 2.9 mm), reflecting a preferential implantation of the heavier isotopes towards the centre of the concentrator target. Precision of the <sup>20</sup>Ne/<sup>22</sup>Ne ratios, expressed as error of the mean, is on average 4‰ (2  $\sigma$ ) for the analyses in which He and Ne were not separated. More work is needed to reduce the considerably larger scatter observed so far in the analyses where He and Ne were separated. The obtained Ne isotope fractionation curve resembles, in shape and extent of fractionation, the post-flight modelled <sup>18</sup>O curve. The two curves are offset by about 10‰. This is probably to be explained by the missing backscatter correction for the measured Ne isotopes. At the conference we will compare measured Ne data with simulated results of Ne implantation at SW conditions prevalent during Genesis collection period.

**References:** [1] Wiens R. C. et al. (2003) Space Sci. Rev. 105, 601-625. [2] Heber V. S. et al. (2006) 37th LPSC abstract, CD #2175. [3] Grimberg A. et al. (2006) 37th LPSC abstract, CD #1782.

**RARE PRESOLAR SILICON CARBIDE GRAINS FROM NOVAE: AN AUTOMATED SEARCH BY NANOSIMS.**

Ph. R. Heck<sup>1</sup>, P. Hoppe<sup>1</sup>, E. Gröner<sup>1</sup>, K. K. Marhas<sup>1,2</sup>, H. Baur<sup>3</sup> and R. Wieler<sup>3</sup>. <sup>1</sup>MPI für Chemie, Partikelchemie, Becherweg 27, D-55128 Mainz, Germany. E-mail: heck@mpch-mainz.mpg.de. <sup>2</sup>Washington University, CB 1105, 1, Brookings Dr., St. Louis, MO 63130 4899, USA. <sup>3</sup>ETH Zürich, Isotopengeologie, NW C84, CH-8092 Zürich, Switzerland.

**Introduction:** The very rare nova grains were traditionally attributed to condense in the ejecta of ONe novae, based on the qualitative agreement of their isotopic composition with models [1,2]. However, we recently reported grain data, which are qualitatively consistent with CO nova model predictions [3]. Another recent study of putative nova grains found supernova-only produced nuclides and hereby excluding a nova origin [4].

Our main goal is to examine the general validity of these findings by applying an automated grain search and analysis technique on a large number of presolar SiC with the NanoSIMS ion microprobe combined with noble gas analyses. C- and N-isotopes are used to identify nova grain candidates, while Ne-isotopes can be used to discern between CO and ONe nova grains. The presence of radiogenic supernova isotopes would exclude a nova origin. At the conference, we will present results of this ongoing study of so far 1089 analyzed presolar SiC grains.

**Samples and Experimental:** Using a standard procedure [5] SiC was extracted from Murchison. The sample preparations and NanoSIMS setup is described elsewhere [3]. Our automated procedure [3,6] primarily consists of the following steps: presputtering to remove surface contamination, raster image (50 x 50  $\mu\text{m}^2$ ) acquisition, particle recognition, single grain analysis. Grains of interest will be analyzed manually for radiogenic supernova isotopes and/or He- and Ne-isotopes. SiC from Murchison and Murray from our first study [7] are also included in the data set.

**Results:** We have found 979 SiC grains from a total of more than 1000 automatically recognized particles. The  $^{12}\text{C}/^{13}\text{C}$  and the  $^{14}\text{N}/^{15}\text{N}$  ratios span the range from 3.7 to 420 and from 26 to 1400, respectively. We classify 19 grains as type A/B, 3 of them having very low  $^{12}\text{C}/^{13}\text{C}$  ratios (<5). Our manual study of 110 presolar SiC grains revealed 5 A/B type grains, with 1 grain having a  $^{12}\text{C}/^{13}\text{C}$  ratio < 5. This gives us 4 out of 1089 grains with particularly low  $^{12}\text{C}/^{13}\text{C}$  ratios, which have  $^{14}\text{N}/^{15}\text{N}$  ratios > 200.

**Discussion and Conclusion:** The C- and N-isotopic compositions of these 4 grains are qualitatively consistent with a CO nova model prediction. For grain SiC070 also the Ne- and Si-isotopic compositions agree qualitatively with this prediction. The analysis of Ne-, Mg- and Ca-isotopes will be diagnostic for the determination of the stellar sources of the grains.

The study of a large number of presolar SiC with our automated search and analyses technique turned out to be efficient. We are confident to discover more nova grain candidates and elucidate their true origin.

**References:** [1] Amari S. et al. 2001. *ApJ* 551:1065. [2] José et al. 2004. *ApJ* 612:414. [3] Heck P. R. et al. 2006. Abstract #1355. 37<sup>th</sup> LPSC. [4] Nittler L. R. and Hoppe P. 2005. *ApJ* 631:L89. [5] Besmehn A. and Hoppe P. 2003. *GCA* 67:4693. [6] Gröner E. and Hoppe P. 2006. *SIMS XV*, in press. [7] Heck P. R. et al. 2005. Abstract #1938. 36<sup>th</sup> LPSC.

**Acknowledgements:** We thank A. Besmehn, S. Merchel and U. Ott for preparing the Murchison residue, J. Huth for his help with the SEM.

### SOLAR NOBLE GASES IN 470 MYR OLD FOSSIL MICROMETEORITES.

Ph. R. Heck<sup>1,2</sup>, B. Schmitz<sup>3</sup>, H. Baur<sup>2</sup> and R. Wieler<sup>2</sup>. <sup>1</sup>Max-Planck Institut für Chemie, Partikelchemie, Becherweg 27, D-55128 Mainz, Germany. E-mail: heck@mpch-mainz.mpg.de. <sup>2</sup>ETH Zürich, Isotopengeologie, NW C84, CH-8092 Zürich, Switzerland. <sup>3</sup>University of Lund, Dept. of Geology, Sölvegatan 12, SE-22362 Lund, Sweden.

**Introduction:** A large abundance of fossil meteorites [1] and sediment-dispersed extraterrestrial chromite grains (SEC grains) [2] have been found in ~470 Myr old marine sediments [3] in quarries in Southern Sweden. Cosmic-ray exposure ages of the fossil meteorites are very short (~0.1–1 Myrs) and increase in younger sediments [4]. The break-up of the L chondrite parent body is thought to be responsible to have caused the high concentration of extraterrestrial matter [1–6]. Since SEC grains are less difficult to find than the fossil meteorites [2,6], our main motivation was to try to determine the exposure ages of the grains.

**Samples and Experimental:** The chromites were extracted from large (10–30 kg) limestone samples with acids, yielding up to a maximum of ca. 3 grains per kg of rock [2]. Grains were hand-picked and identified as extraterrestrial with SEM/EDS (L/LL chondrite composition). Batches of 4–6 chromite grains were weighted (4–8  $\mu\text{g} \pm 10\%$ ) and noble gases were extracted with an IR laser and analyzed in an ultra-high sensitivity mass-spectrometer equipped with a compressor ion-source [7].

**Results and Discussion:** The SEC grains contain very high concentrations (<sup>4</sup>He: 1.4–9.4  $10^{-3} \text{ cm}^3/\text{g}$ ; <sup>22</sup>Ne: 4.9–17  $10^{-6} \text{ cm}^3/\text{g}$ ) of trapped He and Ne. Therefore, the determination of cosmic ray-exposure ages as done for the fossil meteorites [4] was not possible. However, the trapped gases provide clues about the nature of SEC grains. The He- and Ne-isotopic composition of the SEC grains is consistent with solar composition, and noble gas data from stratospheric IDPs [8] and recently fallen micrometeorites [9]. This strongly suggests that also the SEC grains were IDPs and came to Earth as micrometeorites. As we find solar noble gases in all SEC grains from different sediment beds, it is highly unlikely that the grains are fragments of regolith breccias, since only a few percent of all L and LL chondrites are regolith breccias [10]. Model calculations predict that large collisions in the asteroid belt produce so much dust, that the influx of material on Earth increases by two orders of magnitude [11]. Using a simple estimate of the dynamical lifetime ( $t$ ) of dust based on P-R-drag [12] we estimate  $t = 0.6$  to 1 Myrs for 100  $\mu\text{m}$  chromite grains. This is consistent with the delivery times of the fossil meteorites in the same sediment beds [4].

**Acknowledgements:** We thank B. Bottke for helpful discussions and M. Tassinari for participation in the fossil meteorite search. This project has been partly funded by ETH Zürich. Field work was funded by the National Geographic Society.

**References:** [1] Schmitz B. et al. 2001. *Earth Planet. Sci. Let.* 194:1–2. [2] Schmitz B. et al. 2003. *Science* 300:961–964. [3] Trierloff M. et al. 2006. *ESA Spec. Publ.* 612. [4] Heck P. R. et al. 2004. *Nature* 430:323–325. [5] Heck P. R. 2005. Ph. D. Thesis. ETH Zürich. [6] Schmitz B. and Häggström T. 2006. *Met. Planet. Sci.* 3:455–466. [7] Baur H. 1999. *EOS Trans. AGU* 46:F1118. [8] Nier A. O. and Schlutter D. J. 1990. *Met.* 25:263–267. [9] Olinger C. T. et al. 1990. *Earth Planet. Sci. Let.* 100, 77–93. [10] Bischoff A. and Schultz L. 2004. *Met. Planet. Sci.*, 39: 5118. [11] Dermott et al. 2000. In *Asteroids III*:423–442. [12] Burns et al. 1979. *Icarus* 40:1–48.

**DUST IN PROTOPLANETARY DISKS.**

Th. Henning, Max Planck Institute for Astronomy, Königstuhl  
17, D-69117 Heidelberg, Germany. E-mail: henning@mpia.de.

The formation of planets starts with the coagulation process of dust grains. I will summarize observational evidence for this process and will describe the physical processes involved. Infrared and submillimeter observations of the dust emission constrain the timescale of this process.

Infrared spectroscopy has demonstrated that silicate crystals form in disks with properties similar to cometary dust. The crystalline silicates are the Mg-rich end members of the olivine and pyroxene group. The possible formation routes of crystalline silicates in protoplanetary disks will be discussed. New observational tools such as infrared interferometry with long baselines provides direct insight in the spatial variation of dust properties, from the inner few AU of the disks to the outer disks.

**AN OCCURRENCE OF JAROSITE IN MIL 03346: IMPLICATIONS FOR CONDITIONS OF MARTIAN AQUEOUS ALTERATION.**

C. D. K. Herd. Department of Earth and Atmospheric Sciences, University of Alberta, Edmonton, Alberta, Canada. E-mail: herd@ualberta.ca

**Introduction:** Knowledge of the geochemical behavior of K, U and Th is essential in the application of natural gamma-ray spectrometry techniques to Mars exploration. Whereas K, U and Th are expected to behave incompatibly during igneous crystallization, it is difficult to predict whether aqueous alteration will cause fractionation, as it depends on a number of variables such as pH, T, water/rock ratio, etc. This study examines the distribution of K, U and Th between igneous and aqueous alteration phases within a martian meteorite to gain insights into the geochemical behavior of these elements under martian conditions.

**Techniques:** Polished thin sections of MIL 03346 (.93 and .165) from the Antarctic Meteorite Collection were examined using optical, electron microprobe and Synchrotron X-ray methods. A JEOL JXA-8900 electron microprobe (EMP) was used for quantitative (WDS) analysis and X-ray mapping of Fe, Si, S, Al, and K using a spot size of 1  $\mu\text{m}$ . Synchrotron X-ray microprobe mapping failed to detect U and Th, although the technique yielded maps of K, Rb, Sr, Zn, Zr and Fe with a  $\sim 4 \mu\text{m}$  spot size.

**Results:** Iddingsite alteration in olivine, typical for the nakhlites [1] was identified near the edge of an olivine phenocryst and within skeletal olivine in the mesostasis. In both cases, K, S and Fe are enriched and Si is depleted along fractures and grain boundaries associated with the alteration. Preliminary EMP analysis of this material gives  $\sim 5 \text{ wt} \% \text{ K}_2\text{O}$ ,  $1 \text{ wt} \% \text{ Na}_2\text{O}$ ,  $2 \text{ wt} \% \text{ Al}_2\text{O}_3$ ,  $26 \text{ wt} \% \text{ SO}_3$ ,  $50 \text{ wt} \% \text{ Fe}_2\text{O}_3$  and a low total consistent with the presence of OH. Reduction results in a formula broadly consistent with jarosite,  $\text{KFe}_3(\text{SO}_4)_2(\text{OH})_6$ .

**Discussion:** Jarosite has been identified on the martian surface by the Mars Exploration Rover instrument package [2]. Its presence constrains the conditions under which aqueous alteration occurred: jarosite forms in a highly oxidized, acidic ( $\text{pH} < 4$ ) environment [3]. Notably, the jarosite-rich alteration crosscuts the more typical iddingsite alteration, which presumably formed under more neutral conditions. These relationships suggest that the conditions of aqueous alteration changed from neutral to acidic as the hydrothermal system evolved.

Acidic conditions of aqueous alteration favor the mobilization of Th [4]; on this basis the alteration products should have a higher K/Th than the igneous minerals. The crystal structure of jarosite is likely to exclude U and Th [3], and the jarosite in MIL 03346 should therefore have a higher K/U ratio than the igneous minerals. Work is underway to test these hypotheses.

**Acknowledgements:** This study is funded by a Canadian Space Agency contract to MDA Space Missions as part of a Mars Borehole Gamma Ray Spectrometer Concept Study.

**References:** [1] Treiman A. H. 2005. *Chemie der Erde* 65:203-270. [2] Klingelhofer G. et al. 2004. *Science* 306:1740-1745. [3] Papike J. J. et al. 2006. *GCA* 70:1309-1321. [4] Fanghaenel Th. and Neck V. 2002. *Pure Appl. Chem.* 74:1895-1907.

### SOME METHODS TO SYSTEMATICALLY DOCUMENT THE COMPONENTS OF CHONDRITES.

R.K. Herd<sup>1</sup>, P.A. Hunt<sup>1</sup>, and K.E. Venance<sup>1</sup>. <sup>1</sup>Geological Survey of Canada, Natural Resources Canada, 601 Booth Street, Ottawa ON K1A 0E8: [herd@nrcan.gc.ca](mailto:herd@nrcan.gc.ca) , [pahunt@nrcan.gc.ca](mailto:pahunt@nrcan.gc.ca) , [kvenance@nrcan.gc.ca](mailto:kvenance@nrcan.gc.ca) .

**Introduction:** We have recently studied and discussed the textures and mineralogy of recrystallized ordinary chondrites, a carbonaceous chondrite, and primitive ordinary chondrites. We have proposed an atlas of chondrule textures [1,2], to stimulate community interest in the textures of all meteorites and in what they reveal. We here present a framework for precisely locating features within any sample, and we outline an approach to systematically documenting the components of chondrites and their textures, in order to interpret their petrogenesis more rigorously.

**Framework for Locations:** An adaptation of a common and simple means of locating areas of interest in prepared thin sections of rocks is recommended. The lower left-hand corner of a section, photo, or field of view becomes the origin, allowing a cm.-, mm.-, or  $\mu\text{m}$ -scale grid to be superimposed on the whole area. Positions of objects or areas of interest can be noted in (x,y) co-ordinates. During scanning electron microscope or electron microprobe studies, the positions of analytical points can be noted within detailed grids related to less detailed ones. For "mapping" e.g. of back-scattered electron photomosaics, the positions of all components selected for more detailed imaging and analysis can be recorded, along with their dimensions, and their areas can be calculated. The availability of easily reproducible digital images means that basic documentation of this kind should be the first step in examining any prepared materials. The location of objects in 3D within samples can be recorded using an additional co-ordinate (z), representing e.g. the position of a slice of a sample. Thus co-ordinates (1,1,1) represent an area of interest within a slice 1 cm. from the end of a sample, and 1 cm. from the origin along each axis in the prepared section. The equivalent position in mm. is (10,10,10), and in  $\mu\text{m}$ . (10000,10000,10000).

**Systematic Documentation:** The above framework allows us to "leave a trail". Chondrites of all kinds are complex, and analogous to variably melted and recrystallized agglomerations of igneous, sedimentary and metamorphic Earth rocks, each component of which may represent an early Solar System process. We recommend the following: (1) identify lithologies within the section(s) and record their nature, dimensions and position within a grid; (2) treat each lithology as a separate entity, and for each record its components; (3) record the components' size range, modality and primary aspects, e.g. for chondrules, size range and average size, whether certain sizes are predominant, and whether they are rounded, multiple, zoned, fragmental or partial; (4) record the nature of the matrix, and the fusion crust if present (treat as a derivative lithology); (5) use a grid to estimate the percentages of components and matrix; (6) examine e.g. intra-chondrule textures, and contained phases; (7) divide e.g. chondrules into petrographic types, based on contained phases and their textures, presence/absence of mesostasis, and detailed examination of any reaction textures preserved; (8) Interpret the textures as results of processes that may have formed or altered the chondrules and other components; (9) Test interpretations with appropriate analyses; (10) Preserve all data.

**References:** [1] Herd R.K. et al. 2005a. Abstract #2241, 36<sup>th</sup> Lunar & Planetary Science Conference. [2] Herd R.K. et al. 2005b. *Meteoritics & Planetary Science* 40, A65.

### HISTORY OF METAL VEINS IN ACAPULCOITE-LODRANITE CLAN METEORITE GRA 95209.

J. S. Herrin<sup>1</sup>, D. W. Mittlefehldt<sup>1</sup>, and M. Humayun<sup>2</sup>. <sup>1</sup>NASA Johnson Space Center. E-mail: [jason.s.herrin1@jsc.nasa.gov](mailto:jason.s.herrin1@jsc.nasa.gov)  
<sup>2</sup>National High Magnetic Field Laboratory and Dept. of Geological Sciences, Florida State University.

Graves Nunataks (GRA) 95209 has been hailed as the “missing link” of core formation processes in the acapulcoite-lodranite parent asteroid because of the presence of a complex cm-scale metal vein network. Because the apparent liquid temperature of the metal vein (~1500°C) is higher than inferred for the metamorphic grade of the meteorite, questions regarding the vein’s original composition, temperature, and mechanism of emplacement have arisen [1,2]. We have determined trace siderophile element compositions of metals in veins and surrounding matrix in an effort to clarify matters.

We analyzed metals in GRA 95209 in a portion of thick metal vein and adjacent metal-rich (30-40 modal%), sulfide-poor (<1%) matrix by EPMA and LA-ICP-MS for major and trace siderophile elements using methods described by [3]. We also examined metals from a metal-poor (~15 modal%) and relatively sulfide-rich (2-5 modal%) region of the sample.

Kamacite is the dominant metal phase in all portions of the sample. In comparison to matrix metal, vein metal contains more schreibersite and less tetrataenite, and is less commonly associated with Fe,Mn,Mg-bearing phosphates and graphite [2,4]. Vein kamacite contains higher Co, P, and Cr and lower Cu and Ge. These minor variations aside, all metal types in GRA 95209 are fairly homogeneous in terms of their levels of enrichment of compatible siderophile elements (e.g. Pt, Ir, Os) relative to incompatible siderophile elements (e.g. As, Pd, Au), consistent with the loss of metal-sulfide partial melt that characterizes much of the clan. Whatever compositional differences between matrix and vein metal that may have originally existed, they have since largely co-equilibrated to similar restitic trace element compositions.

We agree with [2] that metal veins, in their present state, do not represent a liquid composition. The original vein liquid was much more S-rich and emplaced at correspondingly lower liquid temperatures. Much of the Fe,Ni component solidified in cm-scale conduits while S-rich melts were expelled and continued to migrate by percolation. The higher troilite content in metal-poor regions of the sample results mostly from trapping of a small portion of these melts. The troilite is not remnant primary sulfide.

Strong depletions of W, Mo, and especially Ga (>50%, >60%, and >90% depletion, respectively) in metals of the metal-poor GRA 95209 lithology are localized at scales of 10-100 μm in the vicinity of graphite spherules. These depletions must have occurred below the temperatures at which cm-scale equilibration occurred, and future work will seek to determine their cause.

**References:** [1] Mittlefehldt D. W. and Lindstrom M. M. 1998. *Meteoritics & Planetary Science* 33:A111. [2] McCoy T. J. et al. 2006. *Geochimica et Cosmochimica Acta* 70:516-531. [3] Campbell A. J. et al. 2002. *Geochimica et Cosmochimica Acta* 66:647-660. [4] Floss C. 1999. *American Mineralogist* 84:1354-1359.

### LABORATORY ADSORBED NITROGEN AND NOBLE GASES – ARE WE ON THE SAFE SIDE?

S. Herrmann<sup>1</sup>, S. P. Schwenzer<sup>1</sup>, and U. Ott<sup>1</sup>. <sup>1</sup>Max-Planck-Institut für Chemie, Joh.-J. Becherweg 27, D-55128 Mainz, Germany. E-mail: herrmann@mpch-mainz.mpg.de.

Noble gas measurements are usually carried out using step-wise degassing protocols, whereby the lowest T-step(s) are aimed to remove (and quantify) terrestrial contamination. The influence of grinding [1–3] and acid treatment [4] has already been demonstrated. Further, natural weathering processes are capable of introducing fractionated air into the rocks [5, 6]. To our knowledge no investigation of “pure” adsorption during sample handling has been done. Here we present results from an experiment on San Carlos olivine where we determined the amounts of adsorbed nitrogen and noble gases. We compare these to noble gases found in Martian meteorites.

**Experiment:** A sample of San Carlos olivine was mildly crushed to reduce the grain size, resulting in a range of 0.01 to 1.5 mm. The sample was handled and measured according to our usual procedures: 99.56 mg were wrapped in Pt-foil, loaded into the sample holder and degassed for 24 hrs at 130 °C under vacuum. In a first run, the sample was measured at 250, 400, and 800 °C, after which it was removed from the system. The temperature was low enough to avoid any melting of olivine. The Pt-foil was opened carefully on one side and stored – with the sample inside – in an open sample container. After three weeks the Pt-foil was closed, again loaded into the sample holder, degassed and measured at 250, 400, 600, and 800 °C.

**Results:** The intention was to obtain a sample degassed at the temperatures of interest and to quantify the amount and elemental ratios of nitrogen and noble gases adsorbed during re-exposure to air in the short time span of three weeks.

*Helium and neon.* The light noble gases are at blank level in all temperature steps of both experiments.

*Nitrogen and argon.* In the analysis of the re-exposed sample, 55 % of <sup>36</sup>Ar (corresponding to  $9 \cdot 10^{-11}$  ccSTP/g) and 68 % of N<sub>2</sub> (corresponding to 1.3 ppm) are released in the 600 °C step. Compared to <sup>36</sup>Ar and N<sub>2</sub> concentrations in Martian meteorites, the amounts are small and not expected to compromise the interpretation of bulk sample data.

*Krypton and Xenon.* 75 % and 85 % of <sup>84</sup>Kr and <sup>132</sup>Xe, respectively, are released in the 600 °C step of the re-exposed sample. In contrast to nitrogen and Argon, the released amounts are only by factor of 5 lower than amounts found in Martian meteorites, thus an influence on bulk measurements cannot be ruled out. However, the adsorbed gas is found in the lower T-step(s) only. Fractionation of <sup>84</sup>Kr/<sup>132</sup>Xe is observed to values lower than in water [7] but not as low as elementally fractionated air found in desert weathering products [5, 6].

**References:** [1] Srinivasan B. et al. 1978. *GCA* 42: 183–198. [2] Niemeyer S., Leich D.A. 1976. *Proc. Lunar Sci. Conf. 7th, GCA Suppl. 7*: 587–597. [3] Niedermann S., Eugster O. 1992. *GCA* 56: 493–509. [4] Schwenzer, S.P. et al. 2005. *MAPS* 40 (Supplement): A137. [5] Mohapatra R.K. et al. 2002. *LPSC, XXXIII*. # 1532. [6] Schwenzer S.P. et al. 2003. *LPSC, XXXIV*, Abstr. # 1694. [7] Ozima M., Podosek F.A. 2002. *Noble Gas Geochemistry*, Cambridge.

## BULK COMPOSITION OF CHONDRULES IN CARBONACEOUS CHONDRITES.

D. C. Hezel, H. Palme and R. Kießwetter, Universität zu Köln, Institut für Geologie und Mineralogie, Zülpicherstr. 49b, 50674 Köln, Germany. E-mail: d.hezel@uni-koeln.de.

**Introduction:** The formation conditions and the precursor material of chondrules are still a matter of debate. It is not clear whether chondrules formed as open or closed systems, whether they were molten dust balls or condensed as liquids from a gas or whether and/or to what extent their precursor material was presolar, early solar system processed [e.g. 1], derived from earlier chondrules [e.g. 1] or even from differentiated bodies [e.g. 2,3].

Chondrule bulk compositions provide information about chondrule precursors and are essential for understanding chondrule formation. There is only a limited number of bulk chondrule data available from the literature [e.g. 1,4,5]. We have started a project to determine bulk chondrule compositions with improved accuracy in all types of carbonaceous chondrites (e.g. Efremovka, Allende, Renazzo, Acfer 209, Karoonda, Kainsaz, Vigarano, Acfer 182, Hammadah al Hamra 207, Ishiyevu and a variety of antarctic meteorites) to further constrain chondrule formation and the nature of precursor material.

**Technique:** Bulk chondrule data are obtained by modal recombination of thin section EPMA analyses. Using the procedure of [6,7] allows to quantify uncertainties associated with the analyses.

**Results:** So far we analyzed chondrules in five meteorites; data for 8 Efremovka (CV3) chondrules are fully reduced. Efremovka chondrules have Mg/Si-ratios between 0.77 and 1.49. The mean of all 8 chondrules is with an Mg/Si-ratio of 0.99 superchondritic (CI Mg/Si-ratio is 0.91). Matrix varies in Mg/Si-ratio between ~0.55 and ~0.90 and has a subchondritic mean Mg/Si-ratio of 0.74. Modal abundance of Efremovka matrix is ~39 vol% and of chondrules ~61 vol%. This is used to calculate the bulk Mg/Si-ratio of Efremovka with 0.89, which agrees within analytical errors to the literature data of 0.91 [8]. The superchondritic Mg/Si-ratio of the chondrules is thus balanced by the subchondritic Mg/Si-ratio of the matrix. Similar complementary relationships between chondrules and matrix have been previously described for Renazzo (CR2) [9]. This chondrule-matrix relationship has important implications for chondrule formation models. The chemically complementary system of chondrules and matrix requires that both components formed in the same nebula compartment [10]. This nebula compartment either consisted of physically separate chondrule and matrix precursors, which had their matrix and chondrule specific chemical compositions; or, more probable, this nebula compartment consisted of a homogenous dust from which homogenous dust balls formed, which served as precursors for chondrules. During chondrule formation chondrules then acted as open systems and by exchange with the surrounding gas developed their high Mg/Si-ratios.

At the conference we will present a comprehensive set of chondrule data of all types of carbonaceous chondrites.

**References:** [1] Jones R. H. et al. 2005. *In: ASP Conference Series, Vol.341:251–285*. [2] Bridges J. C. et al. 1995. *MAPS* 30:715-727. [3] Libourel G. & Krot A. N. 2006. *37<sup>th</sup> LPSC*, #1334. [4] Hezel D. C. et al. 2006. *GCA* 70:1548-1564. [5] Russell S. S. et al. 2005. *In: ASP Conference Series, Vol.341:317–350*. [6] Hezel D. C. 2006. Abstract #1668. *37<sup>th</sup> LPSC*. [7] Hezel D. C. 2006. *CaGeo* submitted. [8] Klerner S. 2001 *PhD thesis*, 119p. [9] Klerner S. & Palme H. 1999. *MAPS* 34:A64-A65. [10] Huss G. et al. 2005. *In: ASP Conference Series, Vol.341:701-731*.

**NEODYMIUM, SAMARIUM AND GADOLINIUM ISOTOPIC STUDIES OF LUNAR METEORITES DHOFAR 489 AND NWA 032.**

H. Hidaka<sup>1</sup> and S. Yoneda<sup>2</sup>. <sup>1</sup>Dept. of Earth and Planetary Systems Science, Hiroshima University, Higashi-Hiroshima 739-8526, Japan. E-mail: hidaka@hiroshima-u.ac.jp. <sup>2</sup>Department of Engineering and Science, National Science Museum, Tokyo 169-0073, Japan

**Introduction:** Geochemical studies of lunar meteorites are expected to offer new information that has not been known from the Apollo and Luna missions samples. We report here isotopic compositions of Nd, Sm and Gd of two lunar meteorites NWA 032 and Dhofar 489, and compare the data with those of lunar soils and rocks. Isotopic determination of Nd leads to <sup>147</sup>Sm-<sup>143</sup>Nd and <sup>146</sup>Sm-<sup>142</sup>Nd chronometry to consider early differentiation of the samples from lunar mantle. Isotopic compositions of Sm and Gd are used to characterize exposure history of the samples from isotopic shifts on <sup>149</sup>Sm-<sup>150</sup>Sm and <sup>157</sup>Gd-<sup>158</sup>Gd due to neutron capture effect.

**Samples and Experiments:** NWA 032 is a crystalline mare basalt [1]. Dhofar 489 is an anorthositic breccia with magnesian mafic silicates [2]. Besides two lunar meteorites, two soils, 70002 and 70004, and two rocks, 60626 and 77017 were also used for this study. Each sample weighing 20-80 mg was decomposed by HF+HClO<sub>4</sub>. After evaporation to dryness, the sample was redissolved in 2M HCl. Conventional ion exchange techniques using two column procedures were carried out to chemically separate Nd, Sm and Gd [3]. A Micro-mass VG 54-30 thermal ionization mass spectrometer equipped with seven Faraday cup collectors was used for the isotopic measurements.

**Results and Discussion:** Sm and Gd isotopic shifts provide neutron fluences of  $\Psi=0.53 \times 10^{16}$  and  $2.58 \times 10^{16}$  n cm<sup>-2</sup> for Dhofar 489 and NWA 032, respectively. Small fluence of Dhofar 489 suggests short exposure time and/or deep ejection depth, which is consistent with low concentrations of cosmogenic <sup>10</sup>Be and <sup>41</sup>Ca [4]. On the other hand, large fluence of NWA 032 is consistent with long CRE ages of 226-227 Ma supported by <sup>38</sup>Ar production rate [5].

Dhofar 489 shows a small enrichment of <sup>142</sup>Nd ( $\epsilon_{142Nd}=+0.24 \pm 0.19$ ), even considering neutron capture effect on Nd isotopes. Therefore, the <sup>142</sup>Nd isotopic excess of Dhofar 489 is concluded to be due to decay from <sup>146</sup>Sm. Although the Nd isotopic data of other lunar samples are in progress, <sup>147</sup>Sm-<sup>143</sup>Nd and <sup>146</sup>Sm-<sup>142</sup>Nd systematics of a suit of data from lunar materials may put constraints to construct the model of early differentiation and evolution of lunar mantle and crust [6].

**References:**

- [1] Fagan et al. 2002. *Meteoritics & Planetary Science* 37: 371-394. [2] Takeda et al. 2003. Abstract #1284. 34th Lunar and Planetary Science Conference. [3] Hidaka et al. 1995. *Anal. Chem.* 67: 1437-1441. [4] Nishiizumi et al. 2004. Abstract #1130. 35th Lunar and Planetary Science Conference. [5] Fernandes et al. 2001. *Meteoritics & Planetary Science* 36: A57. [6] Nyquist et al. 1995. *Geochim. Cosmochim. Acta* 59: 2817-2837.

**A POSSIBLE METEORITE LAG DEPOSIT AFTER CONTINENTAL GLACIATION IN SOUTHEASTERN MANITOBA.**

A. R. Hildebrand<sup>1</sup>, M. Beech<sup>2</sup>, S. A. Kissin<sup>3</sup> and G. B. Quade<sup>1</sup>  
<sup>1</sup>Department of Geology and Geophysics, University of Calgary, 2500 University Drive NW, Calgary, Alberta, Canada T2N 1N4; E-mail: ahildebr@ucalgary.ca. <sup>2</sup>Campion College, The University of Regina, 3737 Waskana Parkway, Regina, Saskatchewan S4S 0A2; Department of Geology, Lakehead University, Thunder Bay, Ontario, Canada P7B 5E1.

**Introduction:** Since the discovery that meteorites are concentrated near margins of the Antarctic ice sheet (where stagnation of ice flow occurs due to topographic obstacles and deflation of the ice surface occurs from ablation), many have wondered if other continental glaciers (particularly the large ice masses of the northern hemisphere) produced similar concentrations. Both extant ice caps and the much larger, now-melted Pleistocene continental ice sheets have been considered; no similar situation has yet been found, and the occurrence frequency of sufficient flow stagnation and deflation conditions is unknown.

**Iron Meteorite Recoveries in Southeastern Manitoba:** In Canada surface conditions and recent glacial history have resulted in relatively few meteorite recoveries (68), mostly by farmers on cultivated land. However, extraordinarily, a single individual, Derek Erstelle, has found three weathered iron meteorites in the forested area of southeastern Manitoba (from 1998 to 2005). The three meteorites have been recovered in a triangular area with sides of 30 to 40 km. The meteorites are moderately to heavily weathered (most weathered has portions that are >50% oxide). Two individual meteorites were recovered at one locality, but proved to be petrographically identical. The three specimens from the different localities represent different falls: a coarsest octahedrite of chemical group IAB (kamacite bandwidth  $4.3 \pm 1.3$  mm, n=19), a medium octahedrite (kamacite bandwidth  $1.16 \pm 0.28$  mm, n=15), and a severely deformed octahedrite. The third meteorite recovered was the result of a dedicated search of ~10 days duration.

**Glacial History of Southeastern Manitoba:** Manitoba was entirely covered by the Laurentide ice sheet during the Pleistocene; ice withdrew northwards across southern Manitoba ~11,500 years ago [1]. The glacially shaped bedrock surface is covered with subglacial and periglacial deposits, including basal and ablation tills, outwash sand and gravels, and lacustrine sediments [2]. No topography exists in the region that might have blocked ice flow to create a meteorite concentration analogous to the Antarctic case. However, southeastern Manitoba was the site of a right angle collision of two ice lobes. In the west the Koochiching Lobe flowed SEwards from the Keewatin dispersal centre to collide with the possibly slower-moving Rainy Lobe flowing SWwards from a dispersal centre in the vicinity of Hudson Bay [1,2].

**Possible Meteorite Concentration Mechanism:** That meteorites can be found in forested land with modest searching indicates a concentration mechanism operated in southeastern Manitoba. The damming of the Rainy Lobe against the Koochiching Lobe may have created a meteorite concentration. The recovered meteorites were all found near to, but east of the line of collision.

**References:** [1] Fullerton, D.S. et al.; edited by Fullerton, D.S. 2000. *Misc. Invest. Ser. Map I-1420 (NM-14)*; [2] Sado E. V. et al.; edited by Fullerton, D.S. 1995. *Misc. Invest. Ser. Map I-1420 (NM-15)*.

**WHY DOES ANGRA DOS REIS HAVE AN ANOMALOUS (TYPE B) NIR SPECTRUM?** E. J. Hoffman. Physics Department, Morgan State University, Baltimore, MD 21251, USA (ehoffman@morgan.edu).

Burbine et al. [1] presented near infrared (NIR) spectra for three angrites, meteorites containing pyroxenes with large abundances of Ca, Ti, and Al, noting that of the three, Angra dos Reis gives an anomalous ("Type B") NIR spectrum [2], similar to patterns that appear almost at random in spectra of some terrestrial high-Ca pyroxenes (clinopyroxenes) [3, 4].

Mössbauer spectroscopy, an additional method sensitive to the Fe ions responsible for the pertinent absorption bands, turned up yet another anomalous result for almost all NIR Type B samples among some 40 terrestrial high-Ca pyroxenes: a signature suggesting ferric-ion levels beyond those of chemical analysis [5 and references therein]. A mechanism for this correlation remains elusive, however, and Angra dos Reis does not show this Mössbauer anomaly [5, 6]. Its Mössbauer pattern does suggest  $\text{Fe}^{2+}$  in the octahedral M2 site, though, and Hazen and Finger [7] deemed this fact consistent with the small amount of  $\text{Fe}^{2+}$  placed in that site by their structure refinement (Table 1, AR). Perhaps this 0.018 ions per 6 oxygens is sufficient also to cause the Type B absorption at 2  $\mu\text{m}$ .

To test this hypothesis I am trying to collect other high-Ca pyroxene samples for which an x-ray diffraction structure refinement exists and subject them to NIR spectroscopy. Best would be those with high Ti and Al (fassaïtes) like the principal phase in Angra dos Reis, perhaps the only such pyroxene for which both an NIR spectrum [2] and a structure refinement [7] have been published. I will present NIR results for several well-characterized terrestrial samples sent to the RELAB for spectroscopy, including two kindly supplied by Dr. J. De Grave, Andranondambo (Table 1, M5) and Val di Fassa RA313 (Table 1, RA) [8].

The greatest need is for samples that like Angra dos Reis have a small amount of  $\text{Fe}^{2+}$  in the M2 octahedral site, and I appeal to the mineralogical community to suggest some.

Table 1. Samples Mentioned in the Text

	Cations per 6 Oxygens {M2}{M1}(T)	
AR	{Ca <sub>0.968</sub> Na <sub>0.002</sub> Mn <sub>0.002</sub> Fe <sub>0.018</sub> Mg <sub>0.010</sub> }	[Mg <sub>0.568</sub> Fe <sub>0.205</sub> Cr <sub>0.005</sub> Al <sub>1.161</sub> Ti <sub>0.059</sub> ](Si <sub>1.728</sub> Al <sub>0.272</sub> )
M5	{Ca <sub>0.98</sub> Na <sub>0.03</sub> }	[Mg <sub>0.68</sub> Fe <sup>2+</sup> <sub>0.07</sub> Fe <sup>3+</sup> <sub>0.03</sub> Al <sub>1.16</sub> Ti <sub>0.04</sub> ](Si <sub>1.77</sub> Al <sub>0.23</sub> )
RA	{Ca <sub>0.98</sub> }	[Mg <sub>0.77</sub> Fe <sub>0.21</sub> Al <sub>0.04</sub> ](Si <sub>1.65</sub> Al <sub>0.15</sub> )

References: AR [7]; M5 and RA [8]; neither AR nor RA showed the presence of ferric ion in chemical analysis.

**References:** [1] Burbine T. H. et al. 2001. Abstract #1857. 32nd Lunar & Planetary Science Conference. [2] Gaffey M. J. 1976. *Journal of Geophysical Research* 81:905-920; this report. [3] Cloutis E.A. and Gaffey M.J. 1991. *Journal of Geophysical Research* 96: 22809-22826. [4] Schade U. et al. 2004. *Icarus* 168: 80-92. [5] Hoffman E. J. et al. 2006. Abstract #1215. 37th Lunar & Planetary Science Conference. [6] Mao H.-K. et al. 1977. *Earth and Planetary Science Letters* 35: 352-356. [7] Hazen R.M. and Finger L.W. 1977. *Earth and Planetary Science Letters* 35: 357-362. [8] De Grave J. et al. 2002. *American Mineralogist* 87: 132-141.

**NEW FINDS OF SHATTER CONES IN DISTAL RIES EJECTA, BERNHARDZELL, EASTERN SWITZERLAND**

B. A. Hofmann<sup>1</sup> and E. Gnos<sup>2</sup>. <sup>1</sup>Naturhistorisches Museum der Burgergemeinde Bern, Bernastrasse 15, CH-3005 Bern, Switzerland. E-mail: beda.hofmann@geo.unibe.ch <sup>2</sup>Institut für Geologie, Universität Bern, Baltzerstrasse 1, CH-3012 Bern, Switzerland.

**Introduction:** A thin horizon of impact ejecta comprising angular fragments of upper Jurassic limestone (up to 30 cm in size), fragments of Triassic pelites and shocked quartz grains is known from three outcrops near St. Gallen in eastern Switzerland. The best outcrop is located on the left bank of the Sitter river near Bernhardzell. The impact horizon is hosted by Miocene marls of the Swiss Molasse basin. A zircon-bearing,  $14.4 \pm 0.06$  Ma old tuff [1] stratigraphically located 70 m above the impact horizon constrains the age of the impact layer. At the time of discovery in 1945, the horizon was interpreted as volcanic [2]. The impact nature was recognized in 1973 after the discovery of a limestone block containing shatter cones [3], and a connection with the Ries was made plausible [4] after recognition of high-speed ejection processes. In recent years several blocks of limestone with shatter cones have been found in the best exposure near Bernhardzell, among the new finds is one with particularly well developed shatter cones allowing the measurement of a statistically valid number of angles between striations (V-angle).

**Comparison of Bernhardzell and Steinheim shatter cones:**

A well-preserved Bernhardzell shatter cone has a higher mean V-angle of  $32 \pm 5^\circ$  as compared with samples from the Steinheim basin (6 samples yielded  $13 \pm 2$ ,  $17 \pm 4$ ,  $20 \pm 5$ ,  $20 \pm 2^\circ$ ,  $16.4 \pm 2.2$ ,  $24.7 \pm 5.5$ , all measurements  $17 \pm 5^\circ$ ,  $n = 93$ ). Based on a model that relates the angle between shatter cone striations with increasing distance from the impact center [5], and the fact that the Steinheim shatter cones seem restricted to the central uplift close to the impact center, the larger angles in the Bernhardzell ejecta suggest a different origin. It is thus likely that these samples are derived from a larger distance from the impact center, such as a peripheral position in the Ries crater.

**Ejection processes:** Located at a distance of 160 km from the center of the Ries crater, an ejection velocity of at least  $1.3 \text{ km s}^{-1}$  is required. While this appears possible in case of limestone, processes of ejection of low-strength pelitic rock fragments up to 10 cm in size remain poorly constrained.

**References:** [1] Fischer et al. 1987. Annual meeting of Swiss Acad. Sci., Lucern (Abstract). [2] Büchi, U. & Hofmann, F. 1945. *Eclogae Geologicae Helveticae* 38:337-343. [3] Hofmann F. 1973. *Eclogae Geologicae Helveticae* 66:83-100. [4] Hofmann B. & Hofmann F. 1992. *Eclogae Geologicae Helveticae* 85:788-789. [5] Sagy A. et al. 2004. *J. Geophysical Research* 109(B10209):doi:10.1029/2004JB003016.

**THE TWANNBERG, SWITZERLAND IIG IRON: NEW FINDS, CRE AGES AND A GLACIAL SCENARIO**

B.A. Hofmann<sup>1</sup>, S. Lorenzetti<sup>2</sup>, O. Eugster<sup>2</sup>, F. Serefidin<sup>3</sup>, D. Hu<sup>3</sup>, G.F. Herzog<sup>3</sup>, E. Gnos<sup>4</sup>. <sup>1</sup>Naturhistorisches Museum der Burgergemeinde Bern, Bernastrasse 15, 3005 Bern, Switzerland. E-mail: beda.hofmann@geo.unibe.ch. <sup>2</sup>Physikalisches Institut, Sidlerstr. 5, 3012 Bern, Switzerland. <sup>3</sup>Department of Chemistry, Rutgers University, Piscataway, NJ 08854, USA. <sup>4</sup>Institut für Geologie, Universität Bern, Baltzerstrasse 3, 3012 Bern, Switzerland.

**Introduction:** The first mass of Twannberg (TWI; 15'915 g [1]) was found 1984 in an area marking the limit of the Rhône Valley glacier during the last ice age. Two additional masses (TWII: 2246 g, TWIII: 2533 g) were recovered in 2000 and 2005 on the attic of an old house and in an old mineral collection, respectively. Both locations are within a few km of the original find site. After discovery of the second mass a reinvestigation and comparison with the first mass was initiated.

**Mineralogy and weathering:** As the original find, the newly recovered masses consist of single crystals of kamacite with skeletal, up to 4.5 cm long and a few mm wide inclusions of schreibersite (10.5 wt% Ni). Fracturing follows a second generation of rhabditic schreibersite (17.2 wt% Ni) occurring as very large (several cm) and thin (20 µm) plates. Bulk phosphorous contents based on schreibersite abundance are 1.7 wt% (TWI) and 0.85 wt% (TWII). Troilite is rare. All three masses are covered by a thick rind of oxides containing numerous inclusions of silicate sand grains, identical to those occurring in local glacial till of the Rhône glacier. Fractures following rhabdite plates allow local deep penetration of oxidation products.

**Noble gases and CRE ages:** Noble gas analyses of TW I and II yielded similar results, confirming pairing. <sup>4</sup>He/<sup>21</sup>Ne ratios indicate stronger shielding for TW I than for TW II. CRE ages of 14.4 ± 7.0 (TWI) and 13.0 ± 3.0 Ma (TWII) are atypically low for iron meteorites.

**Cosmogenic radionuclides:** Activities of <sup>10</sup>Be and <sup>26</sup>Al are much lower (by a factor of 40) than those typically encountered in small iron meteorites. The low values are most likely due to heavy shielding.

**Discussion:** Twannberg is a large meteorite with an unusually young CRE age. During weathering, different meteorite fragments resided in glacial till of the Rhône glacier, as indicated by terrestrial mineral grains in the oxide rind. The meteorite fragments were glacier transported for an unknown distance from their location of fall during one or several cold periods.

**References:** [1] Graham A.L. 1986. *Meteoritics* 21:309-313.

### PETROLOGY AND REE GEOCHEMISTRY OF THE LUNAR METEORITE SAYH AL UHAYMIR 300

Weibiao Hsu<sup>1</sup>, Y. Guan<sup>2</sup>, T. Ushikubo<sup>2</sup>, R. Bartoschewitz<sup>3</sup>, A. Zhang<sup>1</sup>, Th. Kurtz<sup>4</sup> and P. Kurtz<sup>4</sup>. <sup>1</sup>Purple Mountain Observatory, Nanjing, China, E-mail: [wbxu@pmo.ac.cn](mailto:wbxu@pmo.ac.cn), <sup>2</sup>Dept. of Geological Sci., ASU, Tempe, AZ 85287, <sup>3</sup>Bartoschewitz Meteorite Lab, Lehmweg 53, D-38518 Gifhorn, Germany, <sup>4</sup>Henckellweg 25, D-30459 Hannover, Germany.

**Introduction:** Sayh al Uhaymir 300 (SaU 300) is a newly recovered lunar meteorite from Oman. It was classified as a feldspathic regolith [1,2]. This meteorite has a Fe/Mn ratio of 71, Al<sub>2</sub>O<sub>3</sub> content of 20.4 wt %, FeO + MgO of 16.7 wt%, and Th of 0.46 ppm [2]. Its chemical composition falls into the range of mingled basaltic-feldspathic breccias [2,3].

**Petrology:** SaU 300 is predominantly composed of fine-grained matrix with abundant mineral fragments and a few polymict breccias (anorthosite, troctolitic anorthosite, noritic gabbro, and anorthositic gabbro). Numerous euhedral to subeuhedral mineral fragments (~ 100 μm) of olivine, anorthite, and pyroxenes are set in the fine-grained matrix. Lithic clasts appear in angular to round shapes and range in size from several hundred microns to a few mm. Glass veins (50 μm wide), FeNi and troilite grains are also observed in the section.

**REE geochemistry:** REE microdistributions in SaU 300 were analyzed with the ASU Cameca 6f ion microprobe. Measurements were carried out in olivine, anorthite, pyroxenes, and apatite within lithic clasts and the fine-grained matrix. Because of the small grain size (< 50 μm) and inclusion, olivine analyses are often contaminated by a small amount of anorthite. After excluding the contribution from anorthite, olivine exhibits a HREE-enriched pattern with Lu at 3-10×CI and Gd at 0.4-0.6×CI. Within the same clast, olivine has relatively homogeneous REEs. REEs vary by a factor of 3 in olivine from different clasts. Anorthite varies significantly in REEs both within clasts and among different clasts. It has a relatively LREE-enriched pattern with a positive Eu anomaly (~ 20×CI). La varies from 0.8 to 22×CI and Y, an analog of HREE, from 0.5 to 8×CI. Both high-Ca and low-Ca pyroxenes were analyzed. They exhibit typical HREE-enriched pattern with a negative Eu anomaly. High-Ca pyroxene has higher REEs (La 3-25×CI, Lu 20-50×CI) than low-Ca pyroxene (Lu 3-10×CI). One anorthositic clast contains an apatite grain (30×150 μm). Apatite has very high REEs with a relatively LREE-enriched pattern (La 2800×CI and Lu 650×CI) and a negative Eu anomaly (Eu 30×CI). It is very similar to apatite from lunar highlands [4] and from the lunar meteorite EET 96008 [5]. Glass veins have homogeneous REEs with a relatively LREE-enriched (La 17×CI, Sm 12×CI), a positive Eu anomaly (Eu 17×CI) and a relatively flat HREE (12×CI) pattern. Its REEs fall into the range of lunar highlands meteorites [5,6].

**Conclusion:** Petrological and geochemical signatures of SaU 300 are in many ways similar to those of lunar highlands meteorites. SaU 300 is primarily a feldspathic regolith breccia with small amounts of mare components.

**References:** [1] Bartoschewitz R. et al. 2005 Abstract #5023, 68<sup>th</sup> Annual Meteoritical Society Meeting. [2] Bartoschewitz R. et al. 2005 Abstract #5024, 68<sup>th</sup> Annual Meteoritical Society Meeting. [3] Korotev R. L. 2005. *Chemie der Erde* 65:297-346. [4] Lindstrom M. M. et al. 1985 *Lunar & Planetary Science Conference XVI*, 493-494. [5] Anand M. et al. 2003, *Geochimica et Cosmochimica Acta* 67:3499-3518. [6] Korotev R. L. 2003 *Geochimica et Cosmochimica Acta* 67:4895-4923.

**SULFIDE VARIATIONS IN CR CHONDRITES.**

Heinz Huber<sup>1,2</sup> and Alan E. Rubin<sup>1</sup>. <sup>1</sup>Institute of Geophysics and Planetary Physics, Univ. of California, Los Angeles, CA 90095-1567, USA. <sup>2</sup>Dept. of Chemistry and Biochemistry, Univ. of California, Los Angeles, CA 90095, USA; [hhuber@ucla.edu](mailto:hhuber@ucla.edu).

**Introduction:** CR chondrites are low in bulk S and Se ( $9.2 \pm 2.2$  mg/g and  $5.0 \pm 0.8$   $\mu$ g/g, respectively) relative to other carbonaceous chondrite groups (e.g., CO:  $\sim 22$  mg/g S, 7.6  $\mu$ g/g Se; CV:  $\sim 22$  mg/g S, 8.5  $\mu$ g/g Se; CM:  $\sim 31$  mg/g S, 12.9  $\mu$ g/g Se). CR chondrites are also low in coarse sulfide (mainly troilite) as indicated by microscopically determined modal abundances (in vol.%): CR ( $1.7 \pm 1.0$ ); CO ( $3.3 \pm 1.2$ ); CV ( $2.1 \pm 0.8$ ). Data from [e.g., 1-4].

A significant fraction of the S in CR chondrites occurs as fine sulfide grains in the matrix. This is indicated by the relatively high abundance of bulk S (22.6 mg/g) and Se (11.4  $\mu$ g/g) in the matrix-rich CR-an chondrite Al Rais [2].

**Analytical techniques:** In order to ascertain the distribution of coarse sulfides in CR chondrites we studied thin sections of 12 CR and CR-an chondrites microscopically: Acfer 097, Acfer 139, Al Rais, Dar al Gani 1004, El Djouf 001, EET 92062, LAP 02342, NWA 1083, Renazzo and three NWA specimens that have not yet been approved by the Nomenclature Committee. We made BSE mosaic maps of the entire thin sections of Acfer 097, Al Rais, El Djouf 001 and LAP 02342. Six of the CR chondrites were also studied by electron microprobe.

**Results and Discussion:** Sulfide in CR chondrites occurs in three principle petrographic settings: (1) Some sulfide is present as submicrometer grains and rare isolated coarse grains (5-40  $\mu$ m) in the matrix. (2) Approximately 10% of the porphyritic chondrules are surrounded by sulfide-rich rims. Sulfide in these rims ranges from 0.2  $\mu$ m particles surrounded by fine-grained silicate to thick patches (20 $\times$ 200  $\mu$ m) connected to thinner (5-30- $\mu$ m-thick) sulfide stringers. Sulfide-rich rims surround both low-FeO (type-I) and high-FeO (type-II) porphyritic chondrules; we did not find any systematic differences in mineral chemistry between chondrules that are surrounded by sulfide-rich rims and those that are not. (3) There are coarse patches (50 $\times$ 100 to 50 $\times$ 400  $\mu$ m) of sulfide within rare porphyritic chondrules. These patches are typically near the edges of their host chondrule.

Chondrules that contain internal sulfide grains also have sulfide-bearing rims. The sulfide-rich rims were formed during remelting, either by the expulsion of sulfide from the interior of a partly molten chondrule or by the addition of fine-grained sulfide-rich dust to the chondrule followed by external heating.

The paucity of sulfide in CR chondrites may be a result of chondrule formation in the CR region having largely ceased prior to the local nebular environment cooling below the temperature ( $\sim 670$  K) where significant condensation of S commenced.

**References:** [1] Dreibus G. et al. 1995. *Meteoritics* 30:439-445. [2] Kallemeyn G.W. et al. 1994. *Geochim. Cosmochim. Acta* 58:2873-2888. [3] Weisberg M.K. et al. (1993) *Geochim. Cosmochim. Acta* 57:1567-1586. [4] McSween H. Y. 1977. *Geochim. Cosmochim. Acta* 41:477-491.

**LAYERED TEKTITES AND ADJACENT SOILS FROM SE THAILAND.**

H. Huber<sup>1</sup> and J. T. Wasson<sup>1,2</sup>. <sup>1</sup>Institute of Geophysics and Planetary Physics and Dept. of Chemistry and Biochemistry, UCLA, Los Angeles, CA 90095-1567. E-mail: hhuber@ucla.edu. <sup>2</sup>Dept. of Earth and Space Science, UCLA.

**Introduction:** During a fieldtrip to SE Thailand in Feb. 2005 we recovered a large mass of layered tektites from an area south-east of Ubon Ratchathani along the Thai-Cambodian-Laotian border. The main purpose of the expedition was to recover tektites and soils from known localities near and far from a small volcanic locality. Several soil profiles were taken for detailed studies on the soil chemistry and mineralogy and to permit a chemical and isotopic comparison with the nearby layered tektites. The goal was to test the hypothesis that the layered tektites are parts of a melt sheet formed when soils were melted [1]. Besides the chemical analysis the soil and tektite samples will be analyzed for Sr and Nd isotopic variations by K. Mezger and T. Kleine and for <sup>10</sup>Be by G. Herzog.

**Analytical technique:** We used instrumental neutron activation analysis (INAA) to determine the major and trace element contents of tektites and soils. Tektites were sawn in solid slabs of ~3 mm thickness, whereas 300-500mg of soil samples were filled in polyethylene vials. Samples along with standard reference material were irradiated and counted in four cycles using high-resolution gamma-ray detectors. These data were combined with INAA data from previous runs [2] including a basalt sample from Ban Kaset Sombun. We then further prepared the soil samples with a 315 µm sieve and made grain mounts to permit characterization with the optical microscope.

**Results and Discussion:** One special focus was laid on the influence of local basaltic material from near Ban Kaset Sombun in order to attempt to determine whether there were parallel variations in tektite and soil compositions, as expected if the tektites formed at their present locations. Past studies have revealed an ultramafic component mixed within the layered tektites as described by [2-3] and also found in microtektites by [4]. Their influence on the soils is clearly visible by a distinct reddish coloring of local material. We included the westernmost layered tektite at Ban Song and a soil profile from the proximate Ban Ta Kao. From there following the major and trace element distribution of the tektites towards the NE (region near Ban Huai Sai we can clearly distinguish the samples from the basalt-rich area as being high in Co, Fe, Ba, Sc and Sr and low in Ca, As, Hf and to a minor extent in Na and Ga. The other elements show either high variations within (Ir, Au) are quite uniform such as the REE, Ta and U.

For some of the layered tektites we could distinguish between the top and bottom surface. Vertical thin sections of the whole tektites reveal their internal structures and layering. The compositional differences in dark layers of 10-300 µm thickness show distinct enrichments in the elements Fe, Mg, Mn and Ca compared to the lighter glass. These layers do not correlate with the bubble rich and bubble poor layers.

**References:** [1] Wasson J.T. 2003. *Astrobiology* 3:163-179. [2] Wasson J.T. 1991. *Earth Planet. Sci. Letters* 102:95-109. [3] Huber and Wasson. 2004. *35<sup>th</sup> Lunar Planet Sci Conf. Abstract* #2110 [3] Glass et al. 2004. *Geochim. Cosmochim. Acta* 68:3971-4006.

**SELENIUM AND SULPHUR DISTRIBUTION IN THE ANOMALOUS CK CHONDRITE EET 99430.**

H. Huber<sup>1</sup>, H. A. Ishii<sup>2</sup>, and S. Brennan<sup>3</sup> <sup>1</sup>Institute of Geophysics and Planetary Physics, University of California, Los Angeles, CA 90095-1567, USA. E-mail: hhuber@ucla.edu. <sup>2</sup>Institute of Geophysics and Planetary Physics, Lawrence Livermore National Laboratory, Livermore, CA 94550, USA. <sup>3</sup>Stanford Synchrotron Radiation Laboratory, Stanford Linear Accelerator Center, Stanford, CA 94025, USA.

**Introduction:** Within a recent study on bulk trace elemental anomalies in carbonaceous chondrites of the Karoonda group (CK), one meteorite was found to be of specific interest [1]. EET 99430 is a CK4 with a quite low chondrule and opaque mineral abundance compared to mean CKs [2]. Still, most of the major and trace element contents show typical CK chondrite values, except for elements affected by sulphide weathering (Ni, Co, Se). It has lost most of its sulphide phases, as represented in the lack of coarse sulphides in the thin sections as well as a depletion in bulk sulphur by a factor of 10 [3]. Former sulphide veins display visible losses in one phase (presumably pentlandite, the most abundant sulphide in CKs) and only left-over grains of pyrite. Nevertheless, the abundances of several siderophile and chalcophile elements, such as Ni, Co, Au and Se were found to be enriched on average by a factor of 2. Since Se is usually considered as a proxy for sulphur contents, the question of S/Se decoupling within this meteorite arose.

**Analytical methods:** We performed reflected-light optical microscopy to determine the sulphide phases. A mosaic of BSE images was made with the UCLA SEM and the phases were determined with the JEOL-superprobe at UCLA. In order to determine the Se and S (and several other elements) distribution within the sulphide-depleted parts of the thin sections EET 99430,11 and EET 99430,6 we performed micro-synchrotron radiation x-ray fluorescence ( $\mu$ -SXRF) spectroscopy in two line scans [4]. The region of the former sulphide vein was scanned in steps of 25 $\mu$ m and the variations of S, Se, Cu, Fe, Zn, Si and Mn extracted from the spectra obtained.

**Results and Discussion:** The sulphide mineralogy in EET 99430 shows occasional occurrences of pyrites and MSS - no pentlandite, violarite or other thiospinel was found in either thin section. These minerals comprise more than 90% of average CK chondrites sulphide minerals. We chose the former sulphide vein as a potential region to explore possible S/Se decoupling, since it has apparently lost parts of its sulphides with only pyrite remaining. The  $\mu$ -SXRF data show a clear trend for the elements S, Se and Cu peaking within the sulphide region, whereas Fe shows basically a flat distribution from the olivine on the side towards the pyrite grains. S and Se are enriched by a factor of 6 compared to the surrounding olivine bearing areas.

First the results show the versatility of  $\mu$ -SXRF in determining Se and S in these low concentrations. Second, Se obviously follows sulphur within this area, so the enrichments in Se may appear within other regions of the meteorite. Further investigations on the source, or rather the reprecipitation areas, within EET 99430 have to be made.

**References:** [1] Huber H. et al. 2006. GCA, in review. [2] Neff K.E. and Righter K. 2006. 37<sup>th</sup> Lunar Planet. Sci. Conf. Abstract #1320. [3] Oura et al. 2004. Antarctic Meteorite Res. 17:172-184. [4] Ishii et al. (2006) 37<sup>th</sup> Lunar Planet. Sci. Conf. Abstract # 2198.

### THE EXPOSURE HISTORY OF THE VERY LARGE L6 CHONDRITE JAH 073.

L. Huber<sup>1</sup>, B. Hofmann<sup>2</sup>, E. Gnos<sup>3</sup>, and I. Leya<sup>1</sup>. <sup>1</sup>Physikalisches Institut, University of Bern, 3012 Bern, Switzerland, E-mail: liliane.huber@space.unibe.ch. <sup>2</sup>Naturhistorisches Museum Bern, 3005 Bern, Switzerland, <sup>3</sup>Institut für Geology, 3012 Bern, Switzerland.

**Introduction:** Large stony meteorites are relatively rare because, in contrast to iron meteorites, they fragment during atmospheric entry, producing large meteorite showers. Surprisingly, many of the large chondrites appear to have complex exposure histories with a first stage exposure on the parent body. In an ongoing study to answer the question whether a complex exposure history is simply more easily detected in large objects or whether they really more likely experienced a complex exposure [1,2] we intensively studied the very large meteorite JaH 073 (L6).

**Experimental:** We analyzed 8 different strewnfield fragments with at least two aliquots each. In addition we took 7 samples from known locations within the main mass (~80 kg) and performed 3 step-wise heating experiments. The samples consisted of one or several chips (100 – 150 mg), free of fusion crust and wrapped in Ni-foil. Prior to analysis the samples were pre-heated to desorb loosely bound atmospheric contamination. We measured He, Ne, and Ar isotopic concentrations.

**Results:** The data for JaH 073 show some very interesting features which are worth to be discussed. First, whereas most of data measured for meteorites so far and most of the model calculations predict a lower limit for  $^{22}\text{Ne}/^{21}\text{Ne}$  of about 1.06, some of our data are clearly below this ratio. Second, in a plot  $^3\text{He}/^{21}\text{Ne}$  vs.  $^{22}\text{Ne}/^{21}\text{Ne}$  all our data are below the empirical correlation line [3], indicating (at first glance)  $^3\text{He}$  and/or  $^3\text{H}$  diffusive losses. However using rather qualitative arguments we suppose that the obvious  $^3\text{He}$  deficits are not due to diffusive losses (neither on earth nor in space). We instead propose that the semiempirical correlation [3] is not valid for very large meteorites. Recent model calculations for lunar surface rocks indicate that for low values of  $^3\text{He}/^{21}\text{Ne}$  the ratios  $^{22}\text{Ne}/^{21}\text{Ne}$  start to increase (at nearly constant  $^3\text{He}/^{21}\text{Ne}$ ) [4]. If true, the data measured by us indicate that JaH 073 was rather a  $2\pi$  than a  $4\pi$  object. Plotting  $^{21}\text{Ne}_{\text{cos}}$  as a function of  $^{22}\text{Ne}/^{21}\text{Ne}$  for JaH 073 fragments and main mass samples indicate, despite of the low range of  $^{22}\text{Ne}/^{21}\text{Ne}$ , that the  $^{21}\text{Ne}_{\text{cos}}$  concentrations vary by more than a factor of 10, giving evidence of a complex exposure history. An interesting result is obtained from the samples taken from known locations of the main mass. In contrast to most model calculations and usual assumptions, which all predict decreasing  $^{21}\text{Ne}$  concentrations with decreasing  $^{22}\text{Ne}/^{21}\text{Ne}$  ratios (for large objects), our data clearly show increasing  $^{22}\text{Ne}/^{21}\text{Ne}$  ratios for decreasing  $^{21}\text{Ne}$  concentrations. A similar result has already been observed of one other meteorite, strewnfield fragments from Gold Basin [1].

To summarize, the new data, together with sophisticated model calculations, indicate that the very often used correlations  $^{21}\text{Ne}$  vs  $^{22}\text{Ne}/^{21}\text{Ne}$  and  $^3\text{He}/^{21}\text{Ne}$  vs  $^{22}\text{Ne}/^{21}\text{Ne}$  are ambiguous for large shielding depths. The new data from JaH 073 therefore help to better constrain physical model calculations.

**References:** [1] Welten et al. 2003. *Meteoritics & Planetary Sciences* 38:157-173. [2] Welten et al 2004, Abstract 2020. 35<sup>th</sup> Lunar and Planetary Science Conference. [3] Nishiizumi et al.1980. *Earth & Planetary Science Letters* 50: 156-170. [4] Masarik et al. 2001. *Meteoritics and Planetary Science* 36: 643-650.

**P-T EQUILIBRATION CONDITIONS FOR LUNAR GRANULITIC IMPACTITES: EVIDENCE FROM APOLLO 15, 16, AND 17**

J. A. Hudgins and J. G. Spray. Planetary and Space Science Centre, Department of Geology, University of New Brunswick, 2 Bailey Drive, Fredericton, New Brunswick, E3B 5A3, Canada. E-mail: jillian.hudgins@unb.ca.

We estimate the pressure and temperature conditions at which seven representative samples of the granulitic impactite suite last. This suite is believed to have formed between the solidification of the lunar magma ocean (~4.4 Ga) and the start of the heavy bombardment period (~4.0) [1]. Therefore, results of this study may shed light on the thermal conditions of the Moon during its first 0.5 Ga of evolution.

Lunar granulitic impactites are complex rocks and are poorly understood. These coherent crystalline rocks were derived from the recrystallization of previously brecciated rocks containing clasts from both the ferroan anorthosite and Mg-suites. They are characterized by 70-80% modal plagioclase, display a clast/matrix structure, are enriched in trace siderophile elements (indicative of meteoritic contamination) and contain virtually no KREEP component. Mineral compositions are homogeneous on a cm scale and are assumed to have been re-equilibrated by the last thermal event [1].

Equilibration temperatures were determined using two-pyroxene thermometry [2] based on Ca, Na, Fe, and Mg concentrations in co-existing orthopyroxene and clinopyroxene crystals. For the seven investigated samples, equilibration temperatures were constrained to be between 850°C and 1050°C. These results are in accordance with previous geothermometric calculations (e.g. [3]) and correspond to the latest episode of re-equilibration between clinopyroxene and orthopyroxene (i.e., the conditions of the last episode of metamorphism and recrystallization).

The low pressure gradient on the Moon (0.05 kbar/km) [4] and the lack of phases sensitive to low pressure variations complicate pressure calculations. We estimated equilibration pressures using two monomineralic (clinopyroxene) geobarometers [5, 6]. One was based on the variation of the structural unit-cell parameters of clinopyroxene with pressure; the other considered the Jd-Di exchange reaction and equilibration temperature. We attempted to calculate pressures based on exchange reactions between mineral pairs (e.g., cpx-ol), but were not successful in obtaining viable results, perhaps because these barometers are calibrated for higher pressure assemblages and have errors of a few kbars. Pressures from the monomineralic barometers were determined to be ~1-2 kbar. These pressures correspond to depths of burial of 20 to 40 km, which represent the mid- to lower-crustal region of the Moon. Surface sampling by Apollo astronauts requires exhumation of the granulitic impactites, presumably by subsequent impact events. Our results indicate that metamorphism was due to burial rather than by juxtaposition with impact melt sheets.

**References:** [1] Warner J.L. et al. 1977. 8<sup>th</sup> Lunar and Planetary Science Conference, pp. 2051-2066. [2] Brey G.P. and Köhler T. 1990. *Journal of Petrology* 31:1353-1378. [3] Cushing J.A. et al. 1999. *Meteoritics & Planetary Science* 34:185-195. [4] McCallum I.S. and O'Brien H.E. 1996. *American Mineralogist* 81:1166-1175. [5] Nimis P. and Ulmer P. 1998. *Contributions to Mineralogy and Petrology* 133:122-135. [6] Ashchepkov, I.V. 2001. *GSA Annual Meeting*. ID 11658.

**Ni-RICH OLIVINE AND A CAI WITH AL-DIOPSIDE IN NWA 2748, LL3.4 ± 0.2.**

R. Hutchison<sup>1</sup> and A. Kearsley. Mineralogy Department, Natural History Museum, London SW7 5BD, UK. <sup>1</sup>E-mail: marobh@bopenworld.com

**Introduction:** Survey of a thin section of NWA 2748, using SEM with EDS, revealed two unusual objects, a 4 mm porphyritic olivine (PO) clast chondrule and a 1.4 mm CAI.

**Ni-bearing olivines:** The PO object has phenocrysts <1 mm in size. Cores are Fo<sub>85±2</sub> with NiO = 0.94 ± 0.10, MnO = 0.26 and CaO = 0.17 (all wt %; means of 17 WD analyses), zoned to Fo<sub>58</sub> with decreasing NiO and increasing MnO and CaO (Table). Euhedral to subhedral chrome spinels, <30 µm, are set in olivine rims, rarely in mesostasis. The spinels, analysed by EDS, have 7–8 wt% MgO and 10–13 wt% Al<sub>2</sub>O<sub>3</sub>, higher than the averages in ordinary chondrites [1]. Charge balance indicates that ~10% of the Fe is Fe<sup>3+</sup>. Mesostasis comprises augite dendrites and feldspathic material, "An<sub>33</sub>".

**Discussion:** The high NiO in the PO cores is unmatched, but the clast chondrule is normal in other respects. Equilibrated CK chondrites have olivines of Fo<sub>70–66</sub> with NiO <0.6 wt% and Mn/Fe wt ratios of 0.006–0.010 [from ref. 2], compared with a mean of 0.018 in the olivines in the clast chondrule. The range of Mn/Fe ratios overlaps that in martian olivines [3]. In a planetary body, several factors control the Fe/Mn ratio, including degree of oxidation, with which it should inversely correlate. The NiO content, however, indicates that the PO chondrule may be the most oxidised igneous object recognised to date, but its Fe/Mn ratios are inconsistent with this and testify to a complex origin.

**Spinel-pyroxene CAI:** It lacks a rim sequence and is semicircular with abraded margins. It consists of subhedral to anhedral Al-diopside, <0.2 mm, with interstitial spinels <30 µm. Diopside has 18–25 wt% Al<sub>2</sub>O<sub>3</sub>, above the range in CAIs in ordinary chondrites, but low TiO<sub>2</sub> (Table) is normal [4]. FeO in spinels increases towards the margin of the inclusion. The diopside combines high Al<sub>2</sub>O<sub>3</sub> typical of CAIs in carbonaceous chondrites with low TiO<sub>2</sub> typical of those in ordinary chondrites.

	1	2	3	4	5	6
SiO <sub>2</sub>	40.00	35.30	0.32	0.60	39.20	--
TiO <sub>2</sub>	--	--	0.64	1.31	1.95	0.39
Al <sub>2</sub> O <sub>3</sub>	0.10	0.12	13.20	10.20	25.00	67.50
Cr <sub>2</sub> O <sub>3</sub>	0.36	0.10	52.70	55.70	--	--
FeO	13.60	35.70	24.40	25.30	--	7.82
MnO	0.22	0.63	0.71	--	--	--
NiO	0.83	0.28	0.60	--	--	--
MgO	46.10	27.60	8.18	7.40	9.92	23.10
CaO	0.13	0.42	--	--	25.20	--
Sum	101.34	100.15	100.75	100.51	101.27	98.81

1–4, PO clast chondrule, 5–6, spinel-pyroxene CAI. 1 olivine core, Fo<sub>86</sub>, and 2, rim, Fo<sub>58</sub>, both are WD analyses. Cr-spinels, 3, in mesostasis, and 4, in olivine rim. 5, Al-diopside, 6, Fe-bearing spinel. 3-6 are ED analyses

**References:** [1] Wlotzka F. 2005. *Meteoritics & Planetary Science* 40: 1673–1702. [2] Noguchi T. 1993. *Proc. NIPR Symp. Antarctic Meteorites* 6: 204–233. [3] Papike J. J. 1998. In *Planetary Materials* 7: 1–11. [4] Brearley A. J. and Jones R. H. 1998. In *Planetary Materials* 3: 188–189.

**FIB-TEM AND SIMS OF AEOLIAN AND GLACIAL ANTARCTIC MICROMETEORITES – EVIDENCE FOR ORIGIN OF “COPS”.**

K. A. Huwig<sup>1</sup>, R. P. Harvey<sup>1</sup>. <sup>1</sup>Dept. of Geological Sciences, CWRU, Cleveland, OH 44106. E-mail: huwig@case.edu.

**Introduction:** Previous TOF-SIMS results have shown a difference in distribution and amount of S, F, H and OH ions between the micrometeorites melted from glacial ice and those collected dry from aeolian traps [1]. The goal of this study was to determine whether the increase in F (and the differences in S, H and OH) was consistently present in more than the one micrometeorite studied at that time and to determine what the host mineral(s) for the anomalous ions is.

**Methods:** The two particles are representatives for glacial (ice recovery) and aeolian trap (recovered ‘dry’) micrometeorites. Both particles are the same as within the study described in [1] and were chosen on the basis of least amount of melting and highest overlapping in mineralogy and appearance.

In addition to these two, ten micrometeorites on the same mount as the glacial micrometeorite and eight from the aeolian mount were analyzed using a CAMECA ims1270 ion microprobe at the IGPP, UCLA. NIST SRM 610 glass was analyzed under the same analytical conditions to record the relative sensitivities of <sup>19</sup>F and <sup>30</sup>Si.

A section from both of the previously analyzed micrometeorites was removed using the focused ion beam (FIB) technique as described in [2]. These sections were then imaged and analyzed using a 200 keV FEI TF20 XT STEM at LLNL and EDX and EELS data were collected.

**Results:** Ion probe analyses have shown that the aeolian micrometeorites had a fluorine content comparable to the glass standard, while the micrometeorites melted out of glacial ice varied highly in fluorine content, but were consistently one or two orders of magnitude higher than both the aeolian micrometeorites and the glass standard.

*FIB-TEM analyses* showed that both the aeolian and glacial particles consist of small spinel and Ol or Px grains with interstitial glass. The grains in the glacial particle were larger, ranging from about 0.1 to 1 μm across, while those in the aeolian particle typically ranged from 10 to 300 nm. Due to the similarity in mineralogy and texture, it is likely that they were very similar before atmospheric entry and experienced a slightly different amount of heating creating the disparity in grain sizes.

The glacial micrometeorite also included a beam sensitive amorphous phase that contained the S seen in [1]. This phase also included C, O, P, Fe, Si, Al, Mg, Ca, Na, Cr and Ni in varying amounts. No crystalline portion of this phase was found, so no positive identification of the phase was possible. These spectra correspond to the “COPS” phase as described by [3]. This phase occupies limited areas around the silicate grains, apparently replacing the glass otherwise found. Also it coats the surface of most of the vesicles within the section. The aeolian particle does not contain this phase.

**Acknowledgements:** Thanks to J. Bradley, Z. Dai, N. Teslich, K. McKeegan and A. Schmidt for instrument time and their expertise. The ion microprobe facility at UCLA is partly supported by a grant from the Instrumentation and Facilities Program, Division of Earth Sciences, National Science Foundation.

**References:** [1] Huwig K.A. et al. 2006. Abstract #2403. 37th LPSC. [2] Lee et al. 2003. *Min. Mag.* 67, 581-592. [3] Enggrand C. et al. 1993. 24<sup>th</sup> LPSC 441-442.

### A TRANSMISSION ELECTRON MICROSCOPE STUDY OF INTERNAL SUBGRAINS IN SiC-X GRAINS.

K. M. Hynes, T. K. Croat, S. Amari, A. F. Mertz, and T. J. Bernatowicz, Laboratory for Space Sciences and Department of Physics, Washington University, St. Louis, MO 63130, USA, khynes@hbar.wustl.edu.

**Introduction:** SiC-X grains comprise approximately 1% of the total presolar SiC population. Based on their isotopic compositions, these rare grains are thought to have a supernova origin [1]. While over 500 SiC grains have been studied by transmission electron microscopy (TEM), these grains were primarily mainstream grains and most have not been studied for their isotopic compositions [2]. Microstructure and phase information have been obtained for only two known SiC-X grains and there have been no previous reports of internal subgrains in them [3]. Here we present preliminary results from TEM studies on four SiC-X grains.

**Experimental:** SiC-X grain candidates from the KJG fraction (3  $\mu\text{m}$  average size) from the Murchison meteorite were located by ion imaging (with the IMS-3f) and subsequently analyzed for their C and Si isotopic ratios with the NanoSIMS to confirm their origin. Four of these grains were then selected for TEM studies. The grains were placed in resin and sliced into  $\leq 100$  nm sections with a diamond ultramicrotome and subsequently studied in a JEOL 2000FX TEM equipped with a NORAN Energy Dispersive X-ray Spectrometer (EDXS).

**Results:** The four selected grains all have large  $^{28}\text{Si}$  excesses ( $-309\% \leq \delta^{29}\text{Si} \leq -187\%$ ;  $-436\% \leq \delta^{30}\text{Si} \leq -329\%$ ), as well as  $^{12}\text{C}/^{13}\text{C}$  ratios greater than solar ( $111\% \leq ^{12}\text{C}/^{13}\text{C} \leq 250\%$ ). EDXS analysis shows that three of the grains have significant amounts of Mg, with Mg/Al ratios of up to  $\sim 0.67$ . The Mg and Al appear to be distributed uniformly, in agreement with previously studied SiC-X grains [3]. Because an insignificant amount of Mg typically condenses within SiC during formation (Mg/Al  $< 0.05$  in mainstream SiCs [4]), the Mg is likely radiogenic  $^{26}\text{Mg}$  from the decay of  $^{26}\text{Al}$ . The polytypes observed thus far in the SiC-X grains are the same as those found in mainstream SiC [2]. Most of the crystal domains analyzed in the SiC-X grains are consistent with the 3C-SiC polytype (79% of mainstream SiC), with a preponderance of  $\Sigma=3$  twins. Also observed was one case of an intergrowth between the 3C-SiC and the 2H-SiC polytypes (17% of mainstream SiC). Unlike mainstream grains, which are predominantly single crystal domains [2], the SiC-X grains are composed of multiple small crystal domains, ranging in size from  $\sim 70$ -200 nm. Five subgrains were found within one of the SiC grains. Three of the subgrains are mainly Fe, with Ni/Fe ratios of  $0.21 \pm 0.07$ ,  $0.19 \pm 0.03$ , and  $0.18 \pm 0.06$ . Significant Ti is seen in the third subgrain, although it is unclear at this time if the Ti is uniformly distributed or is in a separate subgrain. The other two subgrains are Ni-rich, with Ni/Fe ratios of  $1.889 \pm 0.279$  and  $0.41 \pm 0.05$ . Preliminary TEM diffraction data from the Ni-rich subgrains do not appear to be consistent with the metal phases previously observed in subgrains found within presolar graphite [5]. Due to the SiC background, we cannot rule out the presence of Si in these subgrains, and silicides are, indeed, a possibility. Further investigation on the phases of these subgrains is ongoing.

**References:** [1] Amari S. et al. 1992. *ApJ* 394:L43-L46. [2] Daulton T. L. et al. 2003. *GCA* 67:4743-4767. [3] Stroud R. M. et al. 2004. *MAPS* 39:5039. [4] Amari S. et al. 1995. *Meteoritics* 30:679-693. [5] Croat T. K. et al. 2003. *GCA* 67:4705-4725.

### ISOTOPIC ANALYSIS OF THE SUN

T. R. Ireland and M. Asplund. Planetary Science Institute, The Australian National University, Canberra, Australia. E-mail: Trevor.Ireland@anu.edu.au

In order to understand the inventories of different isotopic systems in the solar system, solar isotopic compositions must be determined. Oxygen is particularly notable as there is a 5% range in  $^{18}\text{O}/^{16}\text{O}$  and  $^{17}\text{O}/^{16}\text{O}$  due primarily to the presence of a  $^{16}\text{O}$ -rich reservoir in the early solar system mixing with isotopically normal (as seen from a terrestrial perspective) oxygen. Two popular models for the solar isotopic composition identify these end-members as the most appropriate. A normal composition is suggested by scaling in the solar system where increasingly large bodies (asteroids to Mars and Earth) show a similar  $^{16}\text{O}$  abundance. On the other hand refractory inclusions from the early solar system are interpreted as solar condensates and the elevated  $^{16}\text{O}$  abundance is taken as the solar value.

We have determined the solar oxygen isotopic composition by two means. Firstly, we have measured the isotopic composition of oxygen implanted in Fe metal grains that have little intrinsic lunar oxygen. Secondly we have measured oxygen isotopes from the solar photosphere by observational means.

The oxygen isotopic composition measured from the lunar grains is enriched in  $^{17}\text{O}$  and  $^{18}\text{O}$  by 5.3 ( $\pm 0.3$ )% relative to terrestrial oxygen [1]. This is in good agreement with our new improved measurement of the solar photosphere that indicates  $^{18}\text{O}=+4$  ( $\pm 6$ ) % [2]. The relatively large error limits are also consistent with a normal (terrestrial) oxygen isotopic composition, but do not support a  $^{16}\text{O}$ -rich composition for the Sun.

These observations suggest that the bulk protonebular oxygen isotopic composition differs from the composition of the residual planetary system. Such a situation will arise if there is a difference in isotopic composition between the dust and gas of the primordial molecular cloud. While the planetary system is wholly sourced from the dust component, the Sun also obtains a substantial fraction of its oxygen from carbon monoxide gas. The dust brings the refractory element inventory to the Sun, hence CI chondrites are a good representation of the solar abundances of the non-volatile elements.

### References

- [1] Ireland T.R., Holden P., Norman M.D., and Clarke J. (2006) *Nature* **440**, 776-778.
- [2] Scott P.C., Asplund M., Grevesse N., and Sauval A.J. (in press) *Astronomy and Astrophysics*

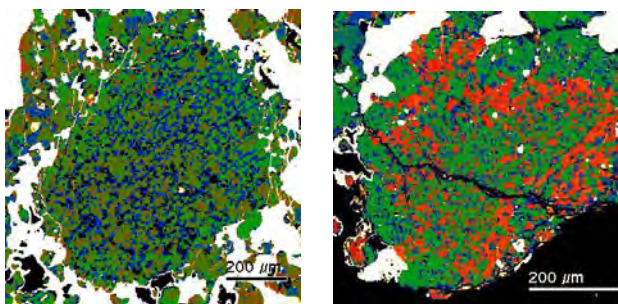
### OXYGEN ISOTOPES IN BRACHINA, SAH 99555 AND NORTHWEST AFRICA 1054

A. J. Irving<sup>1</sup> and D. Rumble, III<sup>2</sup>, <sup>1</sup>Earth & Space Sciences, Univ. of Washington, Seattle, WA, [irving@ess.washington.edu](mailto:irving@ess.washington.edu), <sup>2</sup>Geophysical Laboratory, Carnegie Institution, Washington, DC

**Brachina:** Oxygen isotope analyses by laser fluorination of two whole rock fragments (provided by M. Wadhwa) gave  $\delta^{17}\text{O} = 1.59, 1.38$ ;  $\delta^{18}\text{O} = 3.60, 3.21$ ;  $\Delta^{17}\text{O} = -0.304, -0.307$  per mil. These  $\Delta^{17}\text{O}$  values are more negative than earlier measurements ( $\Delta^{17}\text{O} = -0.20$ ) [1], and also more negative than values for **NWA 595** and **NWA 3151**, which have petrologic characteristics like brachinites [2]. We re-measured NWA 595 after more thorough acid-washing to remove terrestrial oxidation and obtained slightly different results from those we reported previously [2]:  $\delta^{17}\text{O} = 2.11, 2.36, 2.33$ ;  $\delta^{18}\text{O} = 4.33, 4.77, 4.78$ ;  $\Delta^{17}\text{O} = -0.173, -0.162, -0.197$  per mil. **NWA 4042** is petrologically and isotopically similar ( $\Delta^{17}\text{O} = -0.154$ ) [3], and may be related to NWA 595 and NWA 3151 (with  $\Delta^{17}\text{O} = -0.15 \pm 0.02$ ). However, if all these specimens (including Brachina) derive from the same parent body, then it must be isotopically quite heterogeneous.

**Angrite SAH 99555:** Analyses of disaggregated silicate material (provided by T. Kleine) gave  $\delta^{17}\text{O} = 2.20, 2.06$ ;  $\delta^{18}\text{O} = 4.32, 4.06$ ;  $\Delta^{17}\text{O} = -0.077, -0.078$  per mil, which are essentially identical to results obtained for other angrites [4].

**NWA 1054 is not an acapulcoite but a chondrite related to winonaites:** Analyses of material (provided by M. Chinellato via N. Classen) gave  $\delta^{17}\text{O} = 1.56, 1.44$ ;  $\delta^{18}\text{O} = 3.74, 3.54$ ;  $\Delta^{17}\text{O} = -0.408, -0.425$  per mil. We confirm that olivine is  $\text{Fa}_6$  [5] and that chondrules definitely are present (see BSE images). Thus we infer that NWA 1054 is a Type 5 or 6 chondrite related to winonaites not acapulcoites (see [6]), and is likely paired with (or even part of the very same stone as) NWA 725, NWA 1052, NWA 1058 and NWA 1463 (which could usefully be termed “W chondrites”).



**References:** [1] Clayton R. and Mayeda T. 1996) *GCA*, 60: 1999-2018 [2] Irving A. et al. 2005 *MAPS* 40: A73 [3] Connolly H. et al. 2006 *Meteorit. Bull.* 90 [4] Greenwood R. et al. 2005 *Nature* 435: 916-918; Irving A. et al. 2005 *Trans. AGU* 86, #P51A-0898 [5] Moggi-Cecchi V. et al. 2005 *LPS XXXVI*, #1808 [6] Rumble D. et al. 2005 *MAPS* 40: A133.

**MORE AFRICAN ENSTATITE-RICH METEORITES:  
AUBRITE NWA 2828, ZAKŁODZIE-LIKE NWA 4301,  
NWA 1840 AND EL6 CHONDRITES**

A. J. Irving<sup>1</sup>, S. M. Kuehner<sup>1</sup>, T. E. Bunch<sup>2</sup>, J. H. Wittke<sup>2</sup>, D. Rumble, III<sup>3</sup> and G. M. Hupé, <sup>1</sup>Earth & Space Sciences, Univ. of Washington, Seattle, WA, [irving@ess.washington.edu](mailto:irving@ess.washington.edu), <sup>2</sup>Dept. of Geology, Northern Arizona University, Flagstaff, AZ, <sup>3</sup>Geophysical Laboratory, Carnegie Institution, Washington, DC

Several very different types of enstatite-rich meteorites have been found recently in Northwest Africa.

**Aubrite NWA 2828:** Pale gray microbreccia composed mainly of twinned enstatite with subordinate plagioclase (An<sub>13.5-15.3</sub>Or<sub>3-4</sub>) and altered troilite (with daubreelite blades). Rare Mn-alabandite, daubreelite, oldhamite, Ti-free troilite, and very rare kamacite specks are enclosed within enstatite.

**Zakłodzie-Like Enstatite Achondrite NWA 4301:** Mainly twinned pure enstatite with subordinate kamacite plagioclase (An<sub>31-38</sub>Or<sub>1.6</sub>) and troilite with subequigranular igneous cumulate texture (very similar to Zakłodzie [1]).

**Enstatite Achondrite NWA 1840:** Igneous texture with no chondrules; predominantly twinned enstatite with minor maskelynite (An<sub>42</sub>), Si-bearing metal and Cr-rich troilite.

**EL6 Chondrites NWA 3102 and NWA 3134:** Very fresh (W0) paired specimens composed of enstatite (En<sub>98.6-99.3</sub>Wo<sub>1.2-0.6</sub>, 0.16-0.22 wt.% Al<sub>2</sub>O<sub>3</sub>) and metal (1-2 wt.% Si) with subordinate sodic plagioclase (An<sub>9.9-11.9</sub>Or<sub>6.0-4.7</sub>), troilite (Ti-poor, with rare daubreelite blebs), alabandite and fresh oldhamite. Rare partial chondrules are present.

**EL6/7 Chondrite NWA 2965:** Numerous small stones (probably paired with NWA 002 and NWA 1067) evidently are fragments of a very large (>100 kg), broken enstatite-rich meteorite characterized by compression fractures filled with terrestrial limonite and an overall metamorphic texture. We interpret rare round aggregates of fanning prismatic enstatite grains (in 1 out of 4 thin sections) to be recrystallized former RP chondrules. We suspect that **NWA 2736** (classified as an aubrite by [2]) may be part of this same material.

**Oxygen Isotopic Compositions:** Means of replicate analyses by laser fluorination: NWA 2828  $\delta^{17}\text{O} = 2.895$ ,  $\delta^{18}\text{O} = 5.530$ ,  $\Delta^{17}\text{O} = -0.017$ ; NWA 1840  $\delta^{17}\text{O} = 2.793$ ,  $\delta^{18}\text{O} = 5.229$ ,  $\Delta^{17}\text{O} = +0.043$  per mil ( $m_{\text{TFL}} = 0.526$ ). Analyses of NWA 2965, NWA 3134 and NWA 4301 are in progress.

**Conclusion:** We propose that all of these enstatite-rich meteorites originated on the same (fairly large) parent body. As we have argued for the CR parent body [3], there is evidence for a regolith which has been metamorphosed to varying degrees, as well as igneous rock bodies (NWA 011/2400 vs. aubrites) produced by internal partial melting.

**References:** [1] Przylibski T. et al. 2005 *MAPS* 40: A185-A200; Grossman J. 2000 *Meteorit. Bull.* 84; Patzer, A. et al. 2002 *MAPS* 37: 823-833 [2] Lowe J. et al. 2005 *LPS XXXVI*, #1913 [3] Bunch T. et al. 2005 *LPS XXXVI*, #2308.

**GLOBAL CATASTROPHIC CHANGES ON THE TERRESTRIAL PLANETS CAUSED BY LARGE IMPACTS: AN IMPLICATION TO THE PERMAFROST FORMATION ON MARS.**

Isaev V.S.<sup>1</sup> Kondrat'eva K.A.<sup>2</sup>, <sup>1,2</sup> Geological Department, Moscow State University, Vorob'evy Gory, Moscow, Russia, 119899. <sup>1</sup>tpomed@rambler.ru

**Introduction:** A proposal of simultaneous global changing of all terrestrial planets has been made on the basis of a hypothesis of periodical intersection of terrestrial planets of Solar System with intergalactic asteroid flow [1] at the following periods: 3.6, 2.6, 1.65, 1.05 Gyr. This allowed us to find out some analogues between impacts on the Earth, the Moon, Mars as well as on Venus and Mercury and make some conclusions about the age of large impacts for the planets where direct age verification is impossible, as it was made for the Moon [2,3,4,5] and the Earth [6,1].

**Discussion:** The large impact craters influenced the global Earth climate by thermal regime changing, composition and intensity of sediment accumulation [9, 1]. The impactors lead first to the short-term heating of the atmosphere and the surface, then to the long-term cooling that follow to glaciations [6]. Basing on these conceptions and systematization of impacts on the Earth [7,8] we inferred a paleotemperature curve for the Earth. Similar work was made for Mars, where the largest impacts were selected and the closest analogues on the Earth with the determined age have been found. Taking into account present environmental conditions on Mars we made a paleoreconstruction of thermal regime on Mars through its history. Also, some particular features and common elements in the planet evolution were defined and compared with the Earth and the Moon.

**Conclusions:** Due to specific conditions (thin atmosphere, low gravitation and remote position from the Sun) we assume next mechanism of large impacts interaction with Mars. Dust-icy material bringing by celestial bodies and icy material of the surface layers that was excavated by impacts led to the short-period formation of dense atmosphere highly saturated by water and carbonic acid on the planet. This water could be responsible for the appearance of catastrophic fluvial forms on the Martian surface. The cooling, later, due to the low transparency of dusty atmosphere followed to the freezing of short-term water-ice basins. Following accumulation of dust fraction covered the surface by dust layer and preserved water-ice saturated layers from evaporation. This work is supported by fund of RFFI (# 04-05-65110).

**References:** [1] Barenbaum A.A. et al. 2004. Moscow university bulletin. ser.4, Geology, v.3, pp. 3-16. [2] Tera, F., D.A. Papanastassou, and G.J. Wasserburg, 1974, Earth and Planetology Science Letter, v.22, pp.1-21. [3] Swindle, T.D., P.D. Spudis, G.J.Taylor, R.L.Korotev, R.H.Nichols Jr., and C.T.Olinger. 1991. Proceeding of Lunar Planetology Science, v. 21, pp. 167-181. [4] Darliple, G.B., and G.Ryder, 1993. Journal Geophysical Research. v.98, pp. 13,085-13,095. [5] Darliple, G.B., and G.Ryder, ,1996. Journal Geophysical Research., v. 101, pp. 26,069-26,084. [6] Hain V.E. 2003. Second issue. Moscow Nauchnii Mir. p. 337. [7] Feldman V.I. Meteoritika. 1987, vol.46, pp. 154-171.[8] Feldman V.I. Meteoritika. Supplement, 1993. vol.50, pp. 142-145.[9] Abbot D.H., Isley A.E. 2002. Earth and Planetology Science Letters. Vol. 205. p. 53—62. [10] Boynton, W. V. et al. 2002. Science. v. 297, pp. 75-78.

### UNIQUE ZONED CHONDRULES IN THE ISHEYEVO CH/CBb-LIKE CHONDRITE AND THEIR AQUEOUS ALTERATION.

M. A. Ivanova, C. A. Lorenz. Vernadsky Institute of Geochemistry, Kosygin St. 19, Moscow 119991, Russia. E-mail: venus2@online.ru

**Introduction.** The recently discovered Isheyevov CH/CBb-like chondrite consists of FeNi metal, chondrules, CAIs and heavily hydrated matrix lumps which have no genetic relationships with other components [1]. The matrix lumps were the only objects in CH/CBb chondrites which indicate aqueous alteration [2]. However, we found several zoned chondrules surrounded by phyllosilicate rims. Here we report the results of studying of these chondrules and discuss their possible origin.

**Results.** Isheyevov contains chondrules with various textures, including several unusual zoned chondrules, 40-90  $\mu\text{m}$  in size. They consist of magnesian Px or Ol cores and fayalitic rims (Fa60-72) sometimes with small FeNi metal grains. Some chondrules have cryptocrystalline texture in the core and also contain two zones: magnesian in the core and ferrous in the rim with tiny FeNi blebs. Fe/Mn ratios of silicates dramatically change from the core (Fe/Mn - 66 -78) to the rim (Fe/Mn - 141-175) of the chondrules. Similar objects were found in the CHs NWA 470 [3] and Acfer 182 [4]. The chondrule in NWA 470 had even three different zones: MgO-Opx, FeO-Opx, and FeO-Ol. Several zoned chondrules have phyllosilicate rims and magnesian Px or Ol core, sometimes with FeNi metal grains. No any relationships were observed between these phyllosilicate rims and other components of Isheyevov. Phyllosilicate compositions of the rims are in the range of the CMs but differ from the phyllosilicates of the hydrated matrix lumps, which are richer in Mg. FeO content in phyllosilicate rims is similar to that of fayalitic zones.

**Discussion.** The texture and mineralogy of zoned chondrules from Isheyevov, NWA 470 and Acfer 182 indicate a multistage formation. It appears that the core of MgO-rich pyroxene material formed first during condensation. Then the pyroxene grew richer in FeO with decreasing temperature, or fayalite-rich olivine mantle condensed onto the pyroxene core in a region of highly oxidizing conditions. Thus the zones record drastic changes in the physicochemical conditions of the environments where they formed. Phyllosilicate rims either probably were formed from the fayalitic zones of the chondrules in an icy region of the nebula by their reaction with impact-generated  $\text{H}_2\text{O}$ -vapor as proposed by Ciesla et al. (2003) [5], – or the chondrules came from a different asteroid body that had experienced aqueous alteration. Phyllosilicate mantles around chondrules as found in Isheyevov have never previously been reported in CH/CB chondrites. Regardless of the origin of zoned chondrules, their structures must have formed before final accretion of the parent body of Isheyevov as well as all CH and CBb chondrites components (matrix lumps, chondrules, CAIs, FeNi-metal grains) were formed before their accretion into the CH/CBb chondrite parent body.

**References:** [1] Ivanova M.A. 2006. Abstract #1100. 37<sup>th</sup> Lunar & Planetary Science Conference; [2] Krot A.N. et al. 2002. *Meteoritics & Planetary Sciences* 37, 1452-1490; [3] Ivanova M.A. et al. 2001. *Meteoritics & Planetary Sciences* 36, A88; [4] Hezel D. 2002. Abstract # 1787. 33<sup>rd</sup> Lunar & Planetary Science Conference; [5] Ciesla F.J. et al. 2003. *Science*, 299, 549-552.

**CONCENTRIC-ZONED INCLUSIONS IN THE KAUDUN METEORITE.**

M. A. Ivanova, N. N. Kononkova and A. V. Ivanov. Vernadsky Institute of Geochemistry, Kosygin St, Moscow 119991, Russia. E-mail: venus2@online.ru

**Introduction:** The Kaidun meteorite contains a huge variety of different materials formed by multiple processes: 1) nebular condensation, gas metasomatism, agglomeration, nebular melting, 2) asteroidal impact melting, aqueous alteration, and transport of material, and 3) planetary igneous processes typical for large planets [1-3]. Here we report results from Kaidun clast #d6A, which contains many concentric-zoned inclusions formed by processes similar to terrestrial.

**Results.** Clast #d6A is 4 mm in size and consists of phyllosilicates, carbonates and sulfides. It completely lacks anhydrous silicates. The clast has many inclusions with different sizes, textures and compositions. The most interesting of them two concentric-zoned inclusions #d6Aa and #d6Ab. Both inclusions are surrounded by tiny sulfide-phyllosilicate rims. Inclusion #d6Aa consists of serpentine, replaced by talc along its periphery. In the serpentine, FeO and Al<sub>2</sub>O<sub>3</sub> content increase from the center outward to the boundary with talc, while MgO and SiO<sub>2</sub> decrease. The talc is magnesian in composition. Inclusion #d6Ab consists of alternating zones enriched in either calcium carbonates or phyllosilicates (serpentine and chlorite) forming banded structure. The inclusions' cores are mostly carbonates with low Fe and Mg. In the central zones, serpentine and chlorite are present in equal proportions, while chlorite dominates at the periphery. Phyllosilicate compositions from different zones are quite similar.

**Discussion.** The sulfide rims surrounding inclusions in clast #d6A and the absence of anhydrous silicates indicate that it has experienced intense aqueous alteration. A sulfide-enstatite aggregate [4] in direct contact with #d6A suggests the alteration happened before the clast was incorporated into its current location. The serpentine-talc replacement in #d6Aa inclusion appears linked to carbonatization or silicification by Si-bearing fluids below 300°C. The talc composition indicates silicification is more likely. Silicification is usual for contact metamorphism of large masses of ultramafic terrestrial rocks. Talc found in some thermally metamorphosed carbonaceous chondrites is enriched in Al and Na compared with common terrestrial talc. The talc of #dAa compositionally resembles terrestrial magnesian talc. This suggests that the altering fluid for the inclusion, whose talc is similar to terrestrial talc, probably had different composition than the fluid which produced the Al and Na talcs found in metamorphosed carbonaceous chondrites. Inclusion #d6Ab texturally resembles magnesian lime scars of progressive metamorphism and appears to have formed by metasomatic alteration of carbonates by SiO<sub>2</sub>- Al<sub>2</sub>O<sub>3</sub>-bearing fluids below 400-500°C. Given the overall characteristics of Kaidun, we suggest that objects #d6Aa and #d6Ab may have formed in a large, differentiated planet.

**References:** [1] Ivanov A.V. 1989. *Geochemistry International* 26, 84-91; [2] Ivanov A.V. 2004. *Solar Sytem. Research* 38, 2, 150-156. [3] Zolensky M.E., Ivanov A.V. 2003. *Chemie der Erde* 63, 185-246. 1997; [4] Kurat G. et al. 2004. *Meteoritics and Planetary Science*. 39, 53-60.